Evolutionary Optimization of Satellite Formations with Topological Constraints

David Hinckley

Dr. Darren Hitt

Motivation: NASA MMS Mission

NASA's Magnetospheric Multi-Scale Mission (MMS) consisting of a formation of four satellites

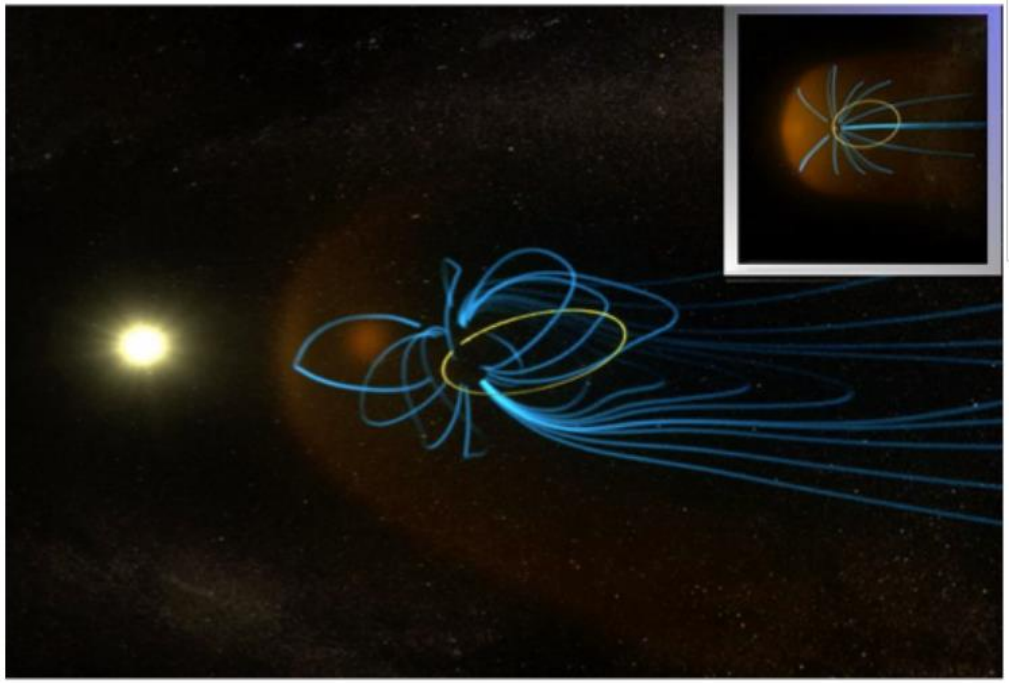

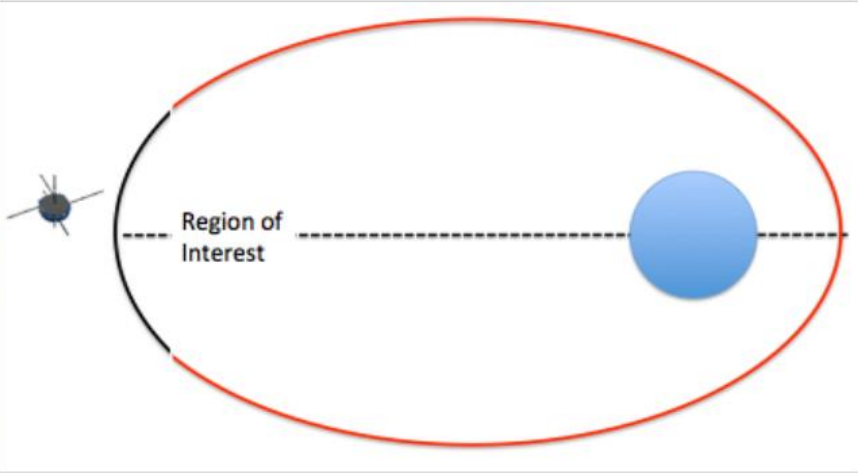

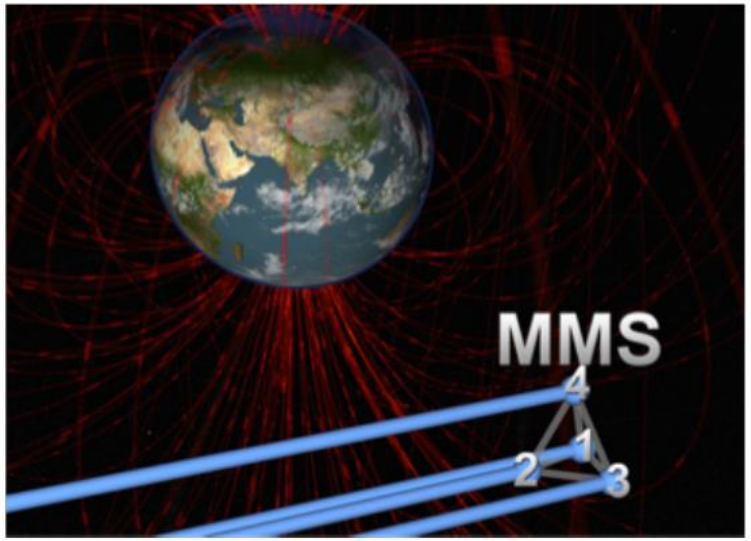

Trajectory Optimization Challenges

- Topological constraints on satellite formation
  - accounting for four satellites
  - “quality” of formation
  - size of formation
- Orbit perturbations
  - oblateness effects
  - atmospheric drag (near perigee)
  - radiation pressure
  - other sources
- Robust design for deployment conditions
  - Location/anomaly
  - Initial configuration

Optimization Strategy – Evolutionary Computing

Conjecture

Owing to the topological constraint on the multi-satellite formation and the system's dynamical complexity, evolutionary approaches for trajectory optimization may be more robust and offer improved performance over classical optimization methods.

Goal of this Study

An evolutionary computing approach is utilized to solving a class of problems involving topological constraints on a satellite formation imposed on a specified region of interest along the reference orbit.

MMS Reference Orbit & Region of Interest

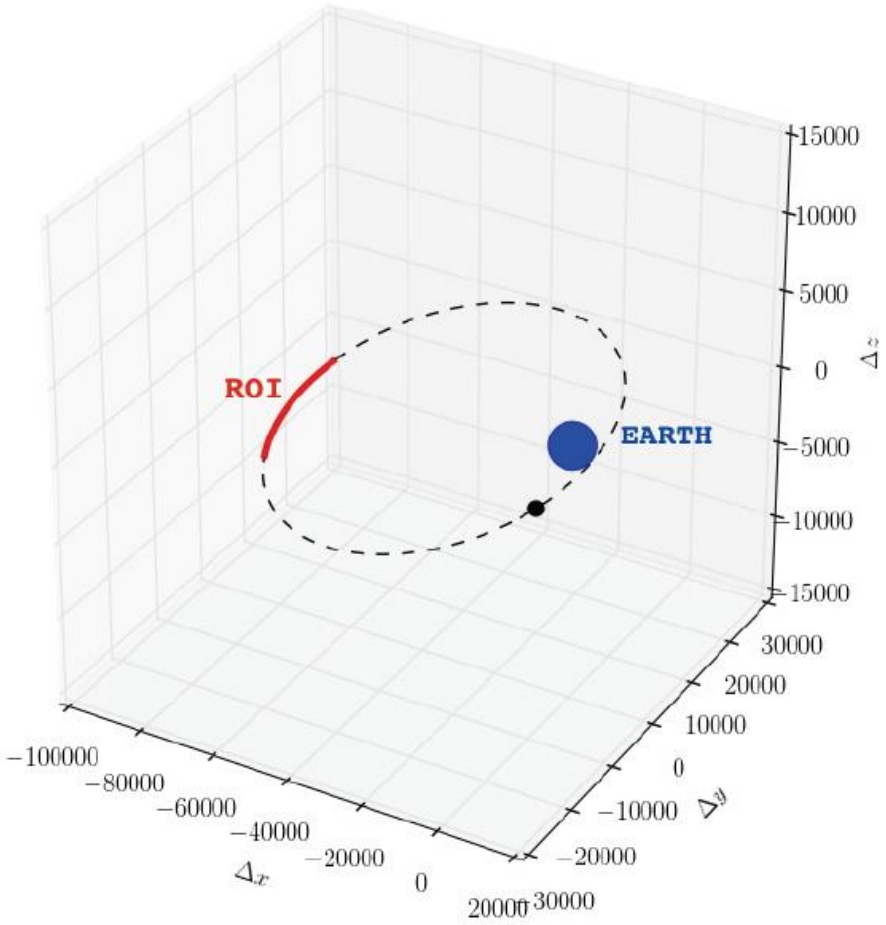

MMS Reference Orbit & Region of Interest (cont'd)

- Perigee 1.2 $R_\oplus$
- Apogee 12 $R_\oplus$
- Eccentricity 0.82
- Inclination 28°
- ROI: ≈ ±20° ≈ ±23,500s centered about apogee
- ≤2 impulsive maneuvers performed at ±90° anomaly; corrective maneuvers at perigee not performed for practical reasons of speed and communication

Evolutionary Algorithms

- Bio-inspired optimization methods that draw upon the concepts of evolution, mutation, recombination, and fitness
- For this problem, candidate solutions are the formation impulse maneuvers
- Differential Evolution is the EA used for this work
- Candidate solutions are made through weighted vector combinations

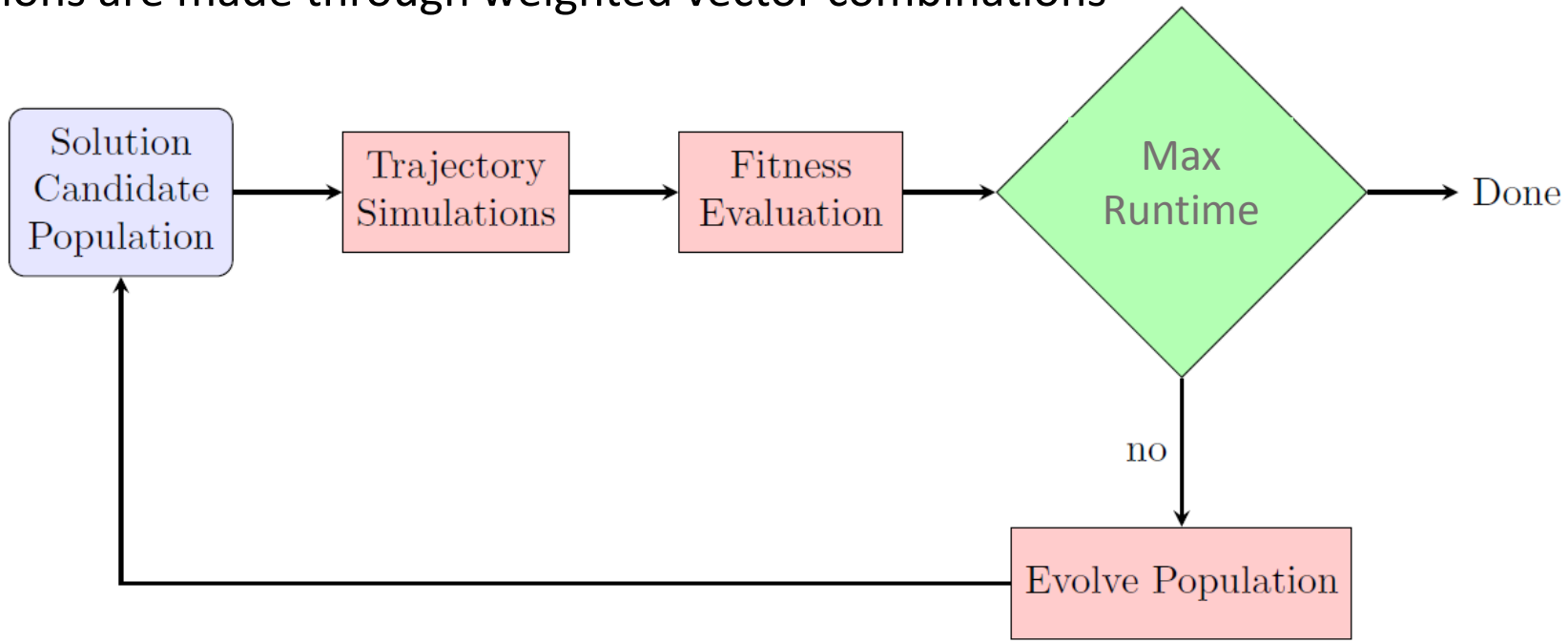

Topological Metrics

- Tetrahedron Quality *Q*

$$Q = \frac{V}{V_{\mathrm{reg}}}, \qquad 0 \leqslant Q \leqslant 1$$

- Average Tetrahedron Side-Length *L*

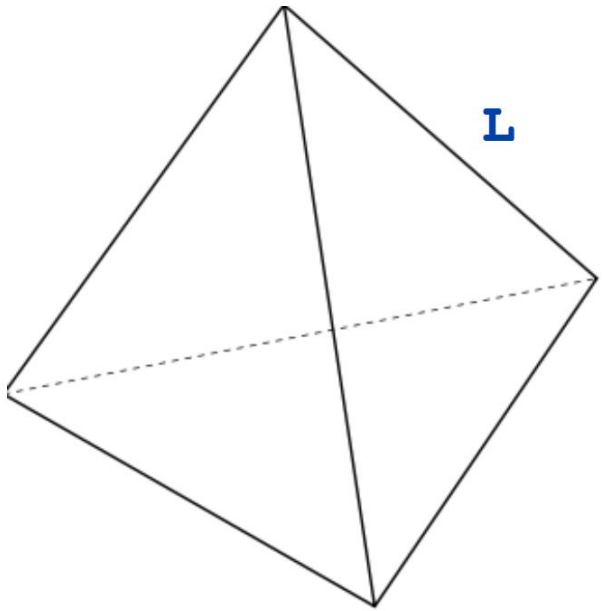

- "Fitness" is a weighted balance of

  Q and *L*

Test Cases

Case 1: MMS orbit; linear deployment configuration at -90° true anomaly

- Linear separation pf 100 m
- Target *L* of 10 km and 160 km
- Impulses performed at ±90°

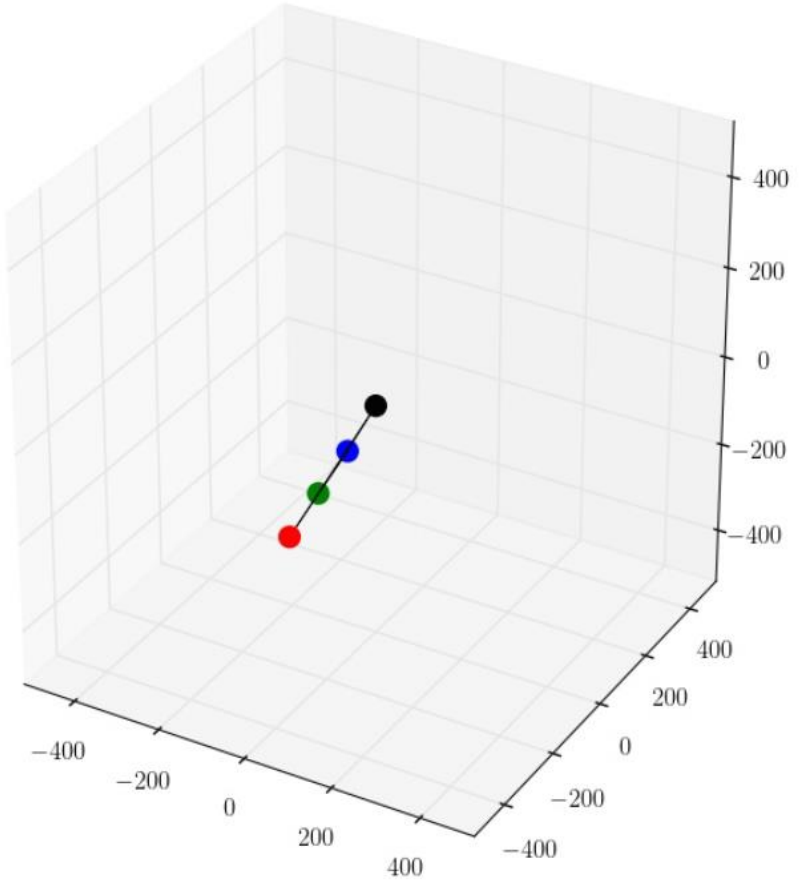

Sample Result

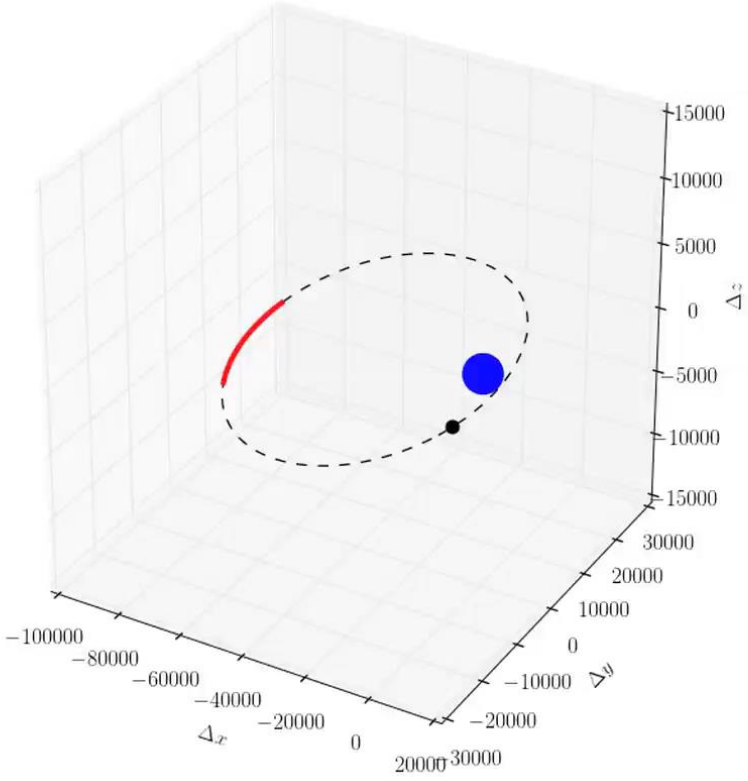

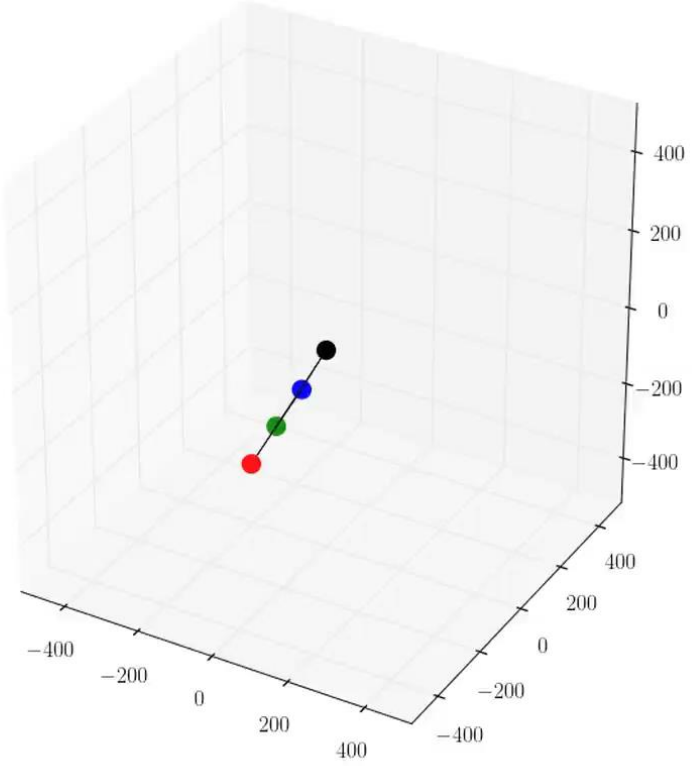

Test Cases (cont'd)

Case 2: MMS orbit; tetrahedral deployment configuration at -90° true anomaly

- Regular tetrahedron configuration
- Impulses performed at ±90°
- Target *L* of 10 km and 160 km
- Initial *L* of 6 km and 130 km

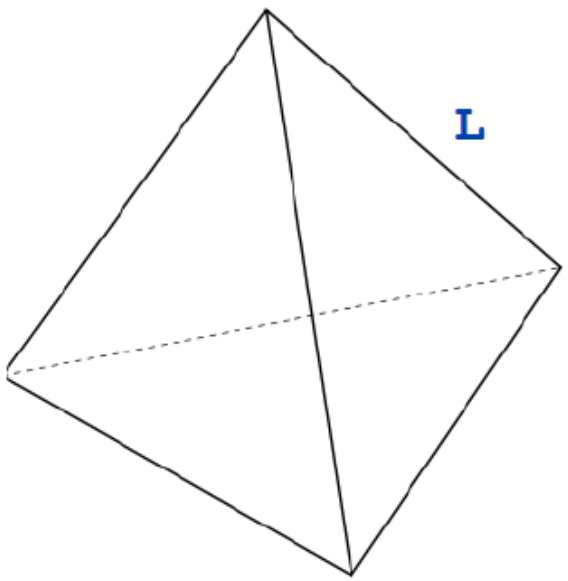

1-Impulse vs. 2-Impulse (Quality)

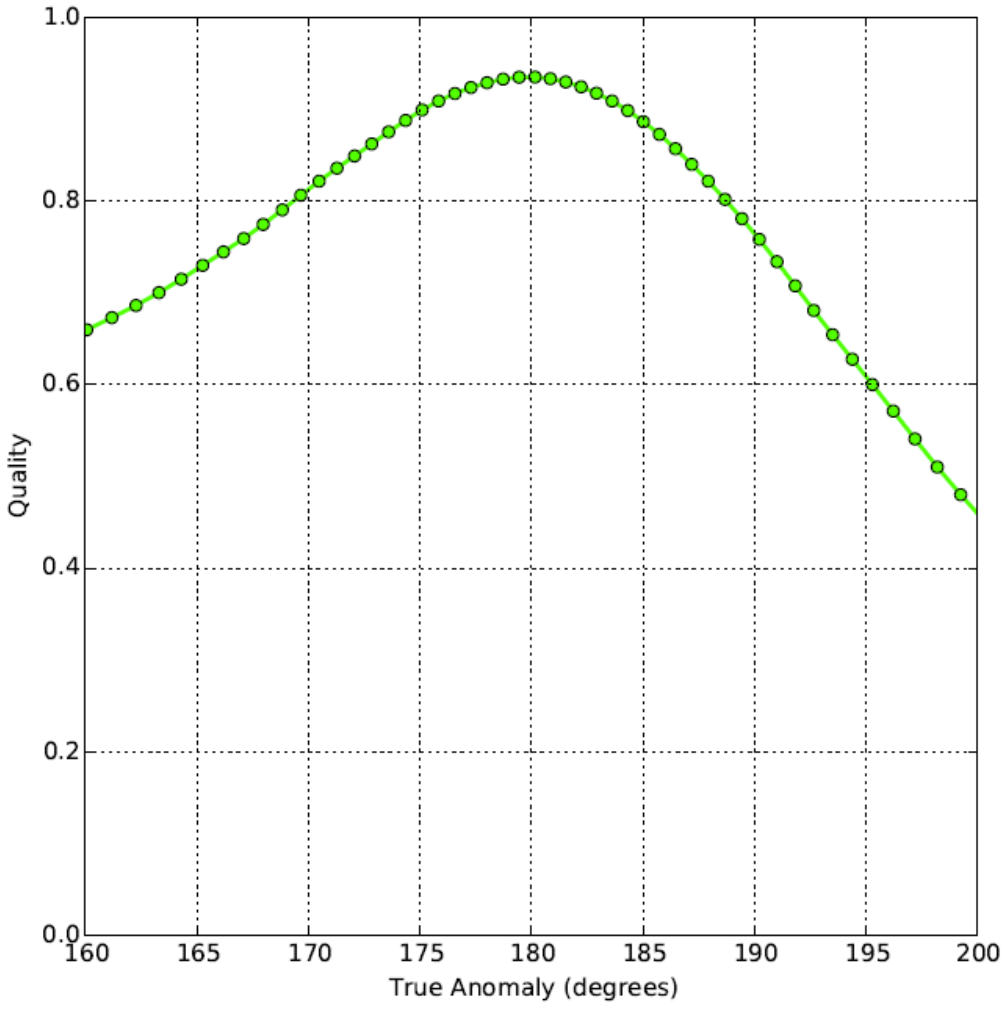

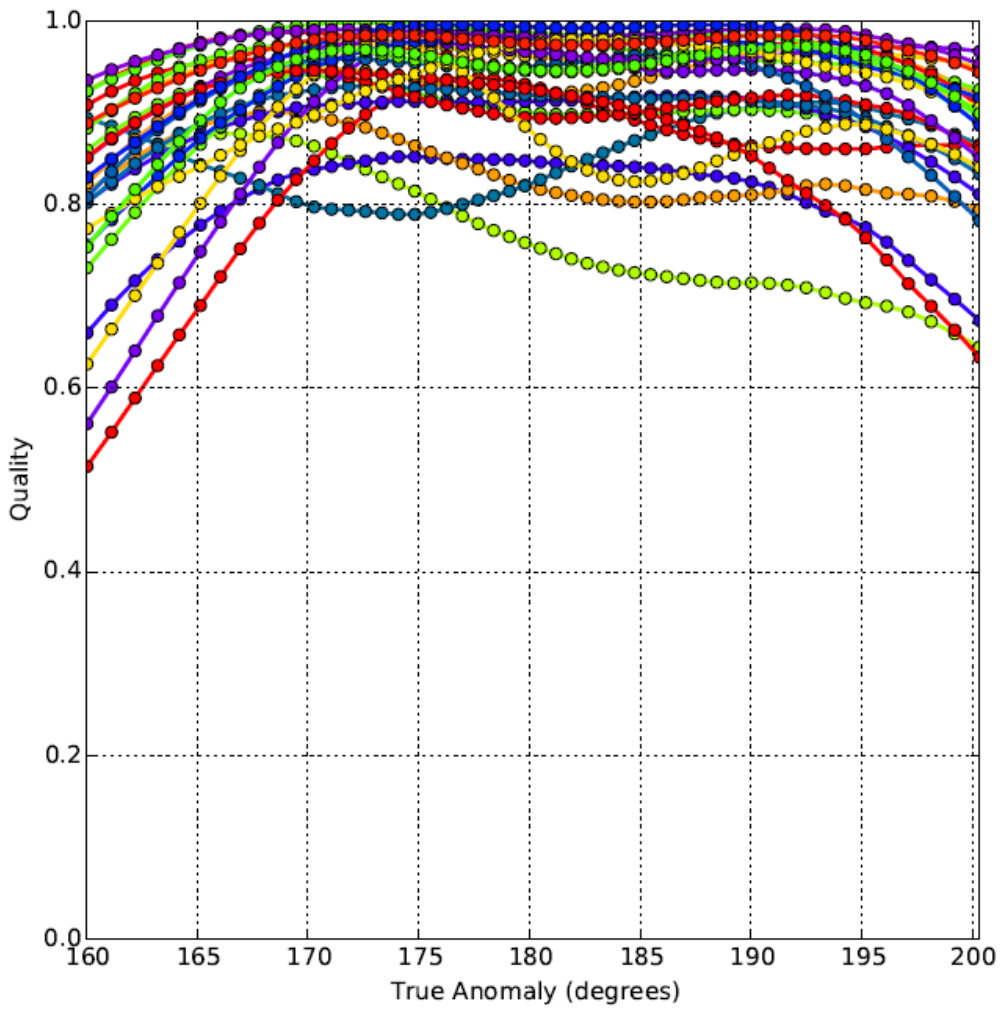

1-Impulse vs. 2-Impulse (Average Side-Length)

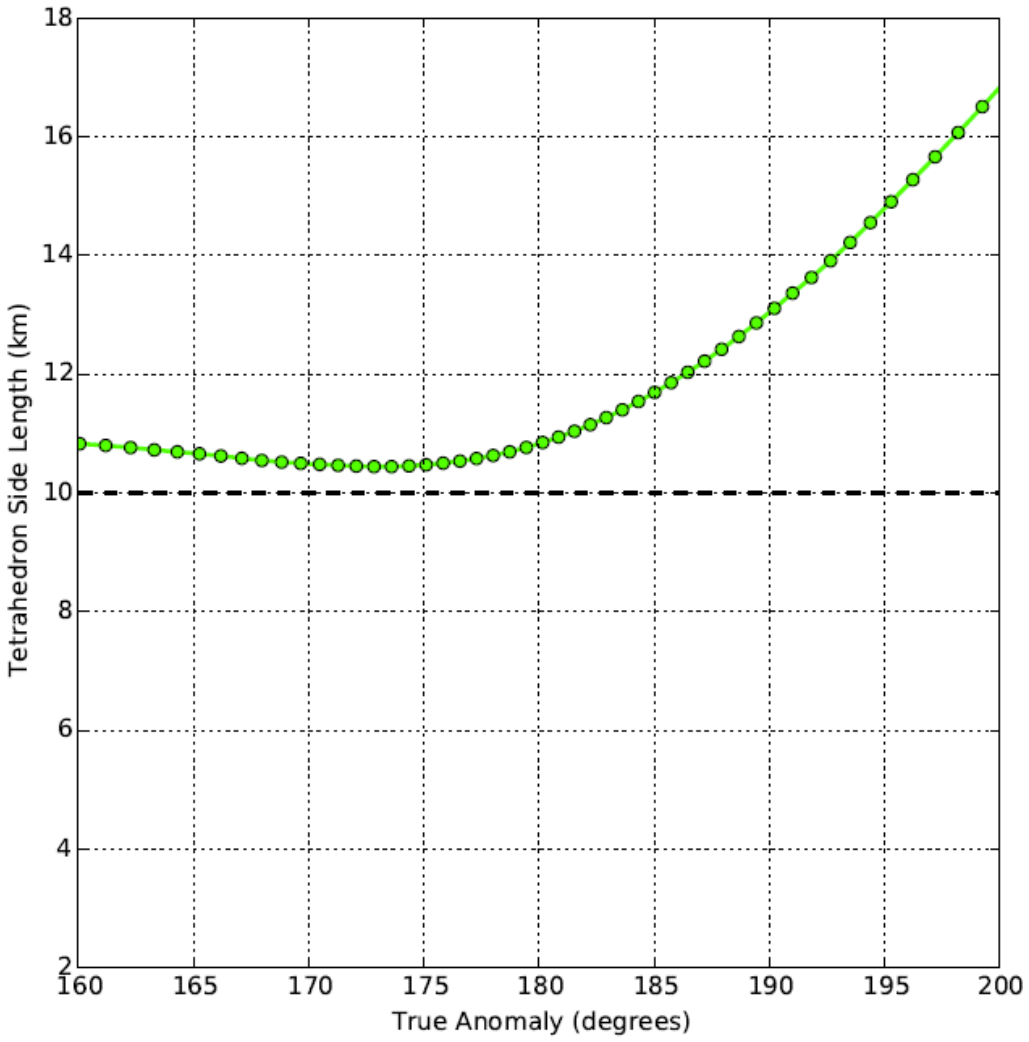

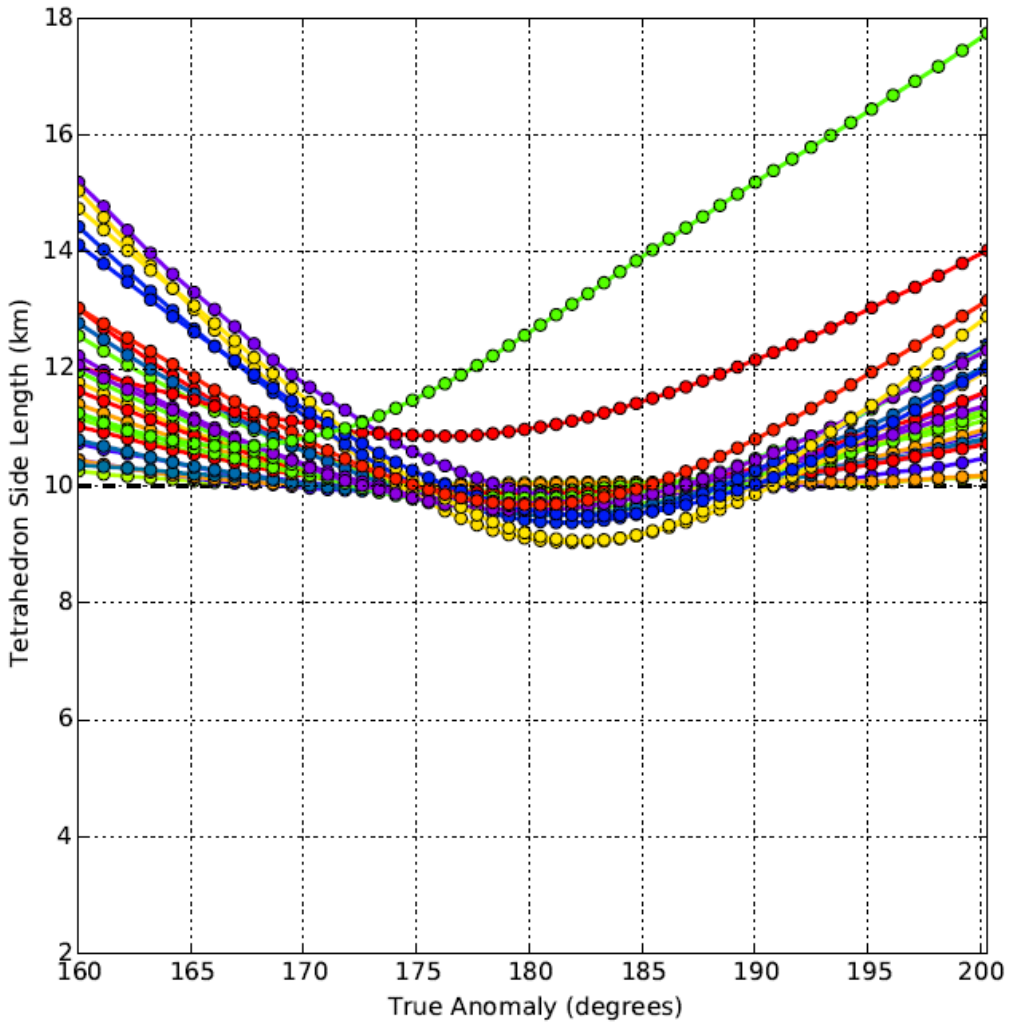

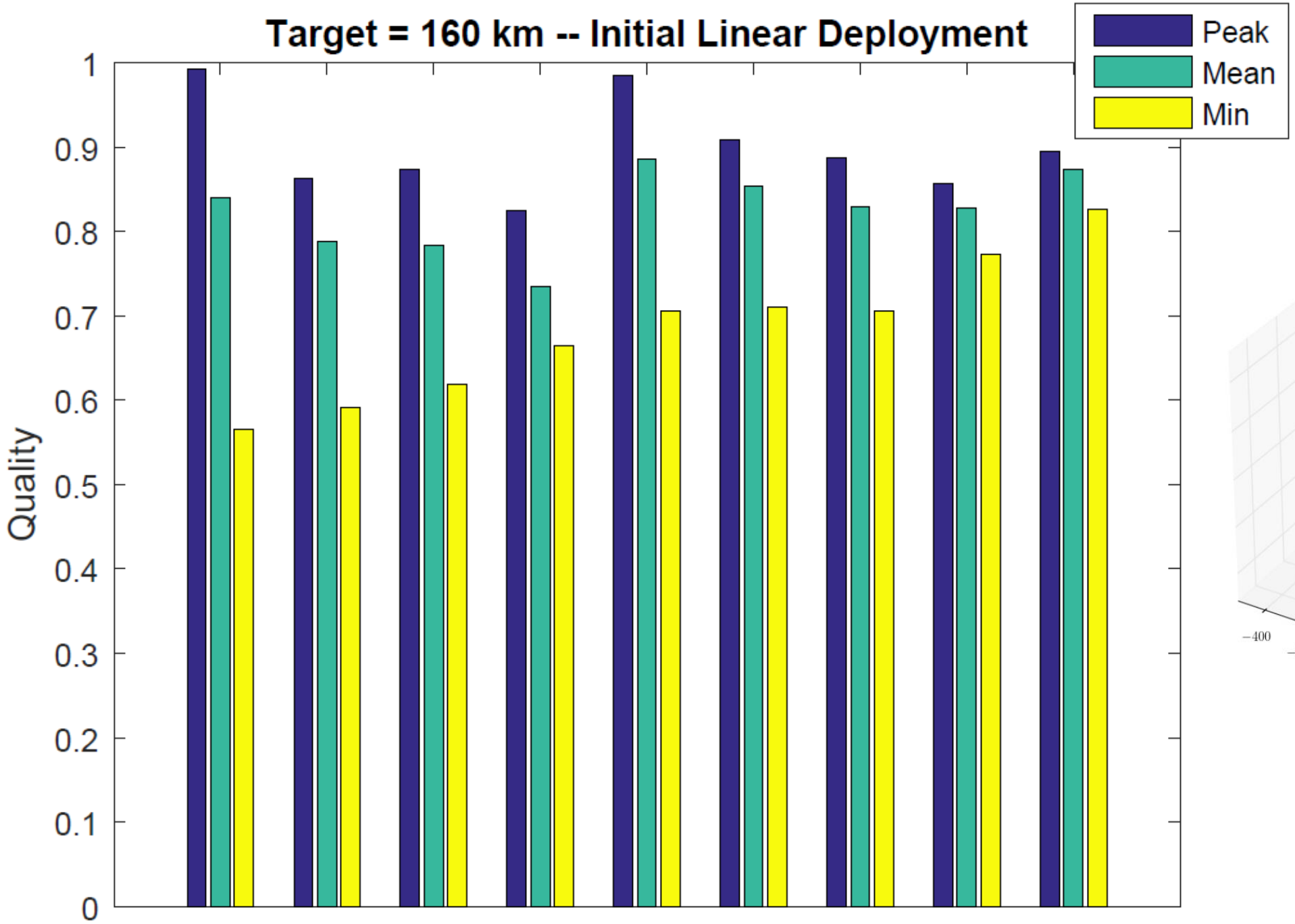
Target = 160 km -- Initial Linear Deployment
Peak
Mean
Min
Quality
1
0.9
0.8
0.7
0.6
0.5
0.4
0.3
0.2
0.1
0

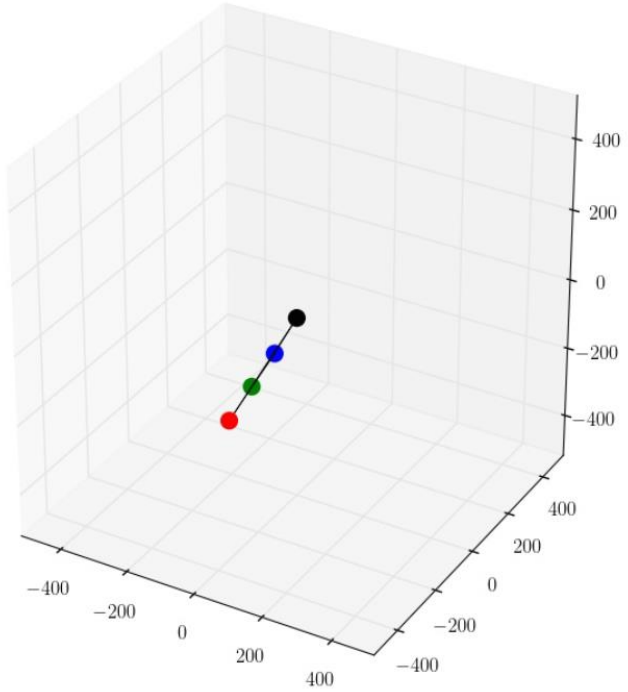
400
200
0
−200
−400
−400
−200
0
200
400
400
200
0
−200
−400

Formation Comparison – Highest Peak vs. Lowest Deviation

Highest Peak Quality

Quality = 0.99

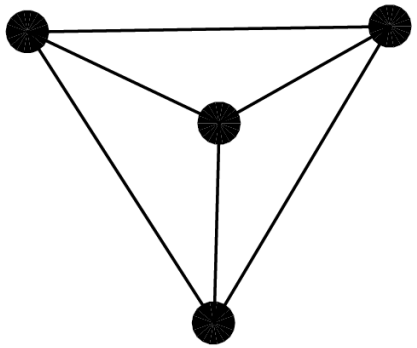

Quality = 0.56

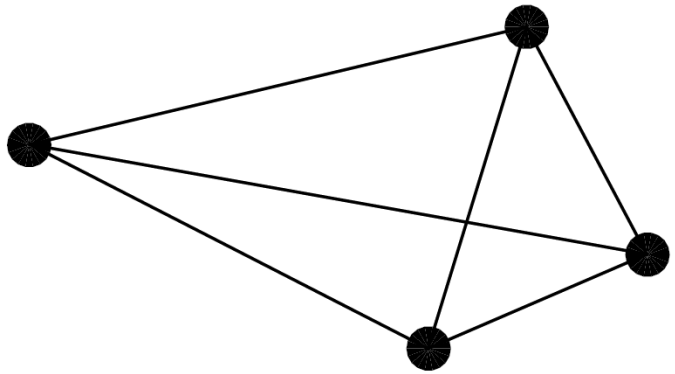

Lowest Quality Deviation

Quality = 0.90

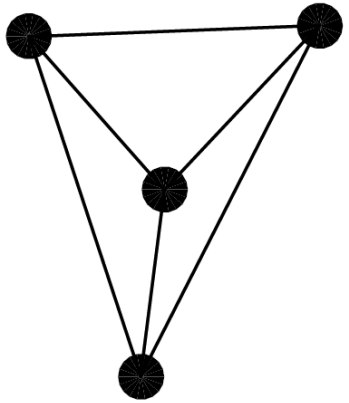

Quality = 0.83

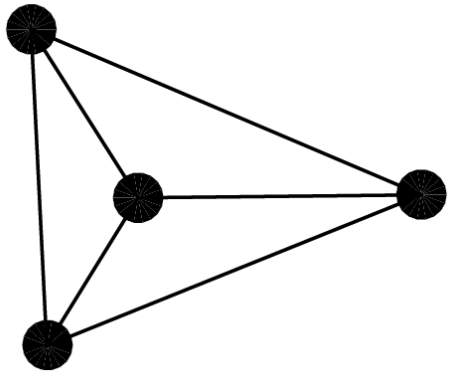

QUESTIONS?

Efficient Cyclization Methodology for Biologically Relevant Precursors

Rachael Carmichael

National space grant director's meeting

March 2016

Sustainable Chemistry

Increased focus on minimizing hazardous chemical waste and cost reduction.

- **Build complexity with as few steps as possible**
  - **Design tandem or cascade reaction sequences**
- **Consider environmental impact**
  - **Simplify purification process**
  - **Eliminate toxic or heavy metals**

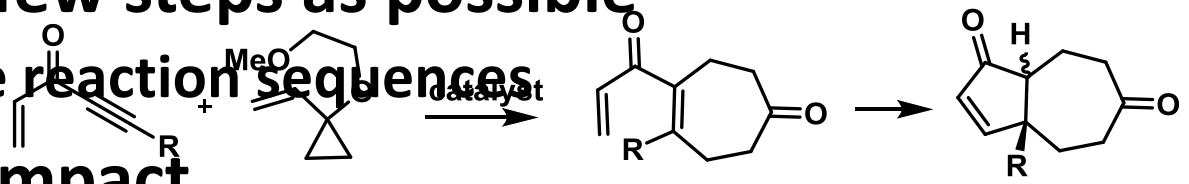

(1)

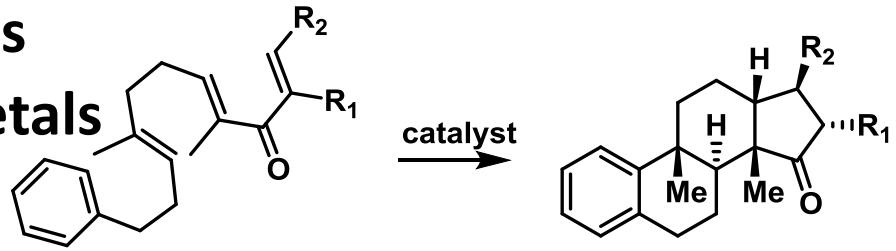

(2)

Wender, P. A., Stemmler, R. T. & Sirois, L. E. *J. Am. Chem. Soc*. **2010**, *132*, 2532–2533. Bender, J. A., Arif, A. M. & West, F. G. *J. Am. Chem. Soc*. **1999**, *121*, 7443–7444.

Interesting [6-5-6] Core

- **Target an important class of biologically active molecules having a common framework**

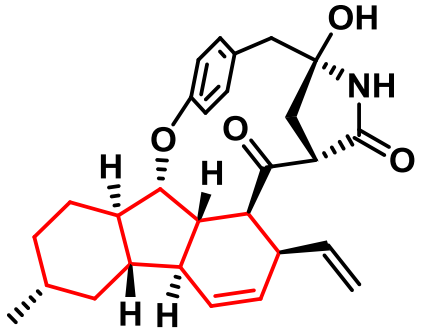

hirsutellone B

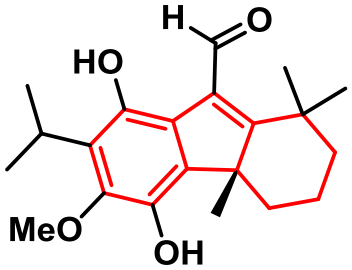

taiwaniaquinol D

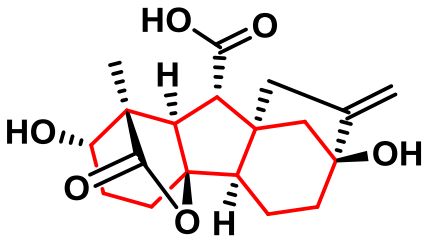

gibberellic acid

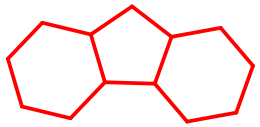

[6-5-6] - carbotricyclic skeleton

- **Develop method to efficiently synthesize [6-5-6] skeleton**
  - **Readily access pertinent natural products and their derivatives**

K. C. Nicolaou, D. Sarlah, T. R. Wu, W. Zhan, *Angew. Chem*. **2009**, *121*, 7002–7006. M. Ozeki, M. Satake, T. Toizume, S. Fukutome, K. Arimitsu, S. Hosoi, T. Kajimoto, H. Iwasaki, N. Kojima, M. Node, et al., *Tetrahedron* **2013**, *69*, 3841–3846. C. R. André Luís Lopes da Silva, Pak. *J. Bot*. **2013**, *45*, 2057–2064

Tandem Diels-Alder Nazarov Cyclization

- **Diels-Alder cyclization**
  - **Awarded Nobel prize in 1950**

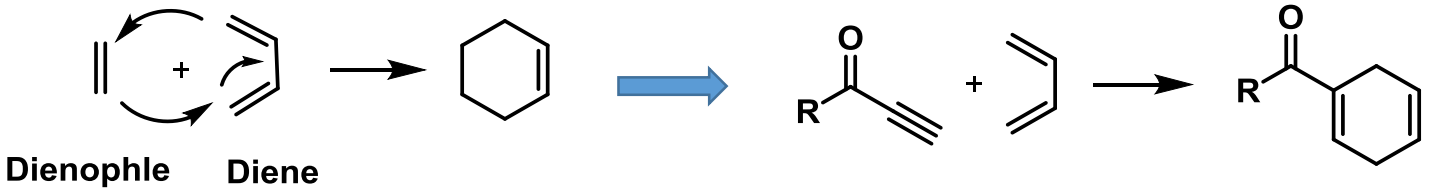

- **Design route towards [6-5-6] advanced intermediates**
  - **Utilize diynone starting materials as the dienophile**

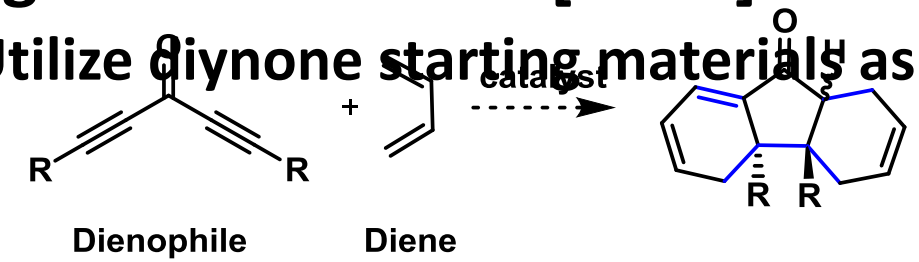

Diels, O; Alder, K. *Liebigs Ann. Chem*. **1928**, *460*, 98. Corey, E; Lee, T. *Tetrahedron Lett*. **1997**, *38*, 33, 5755

Regio-control Through β–silyl Effect

Proposed mechanism:

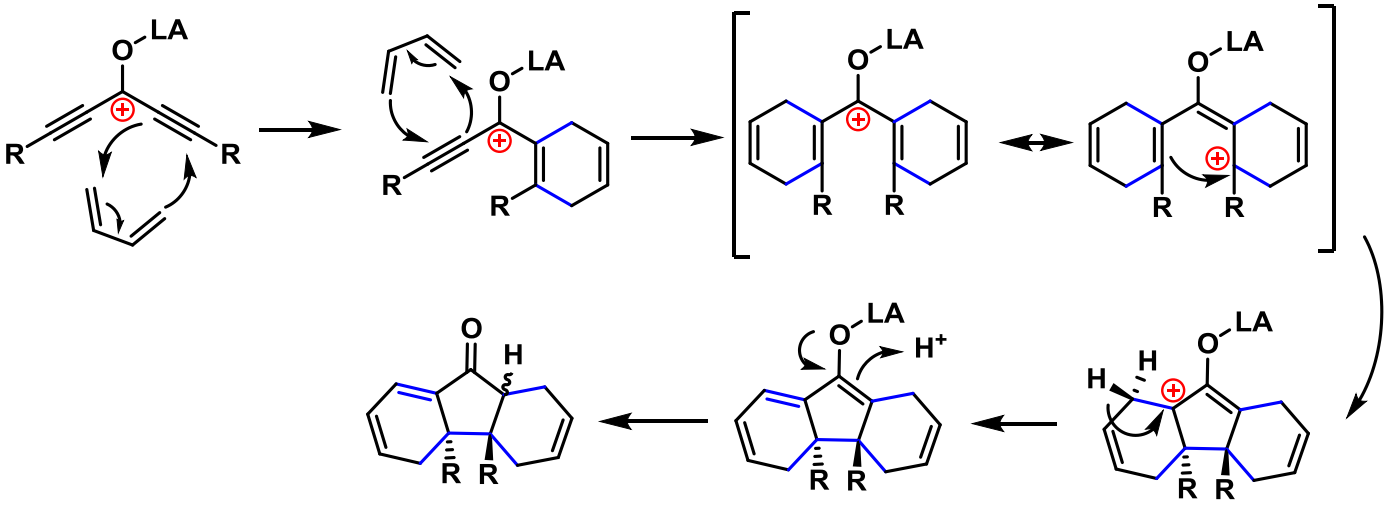

Elimination of silyl group allows for control over double bond location.

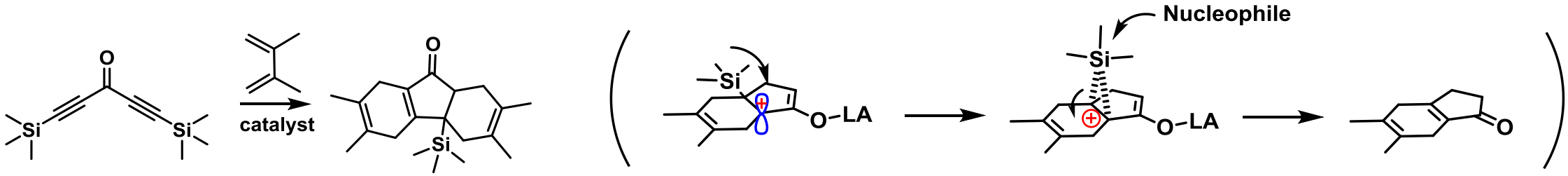

simplified reaction scheme for clarity

Catalyst Screening

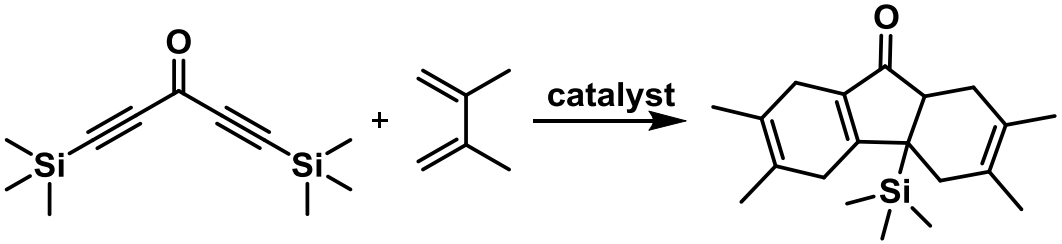

Catalyst	T (°C)	t [h]	Yield [%]
$ZnCl_2$	23	9	0
$BF_3 \cdot Et_2O$	-17	2	0
$SnCl_4$	-78	1	0
$TiCl_4$	-78	2	0
$FeCl_3$	0	1	0
$AlCl_3$	0	40	30
$EtAlCl_2$	23	30	64
Me_2AlCl	**23**	**1.5**	**78**
$In(OTf)_3$	23	1	0
BCl_3	-5	10 min	58

Major Isomer

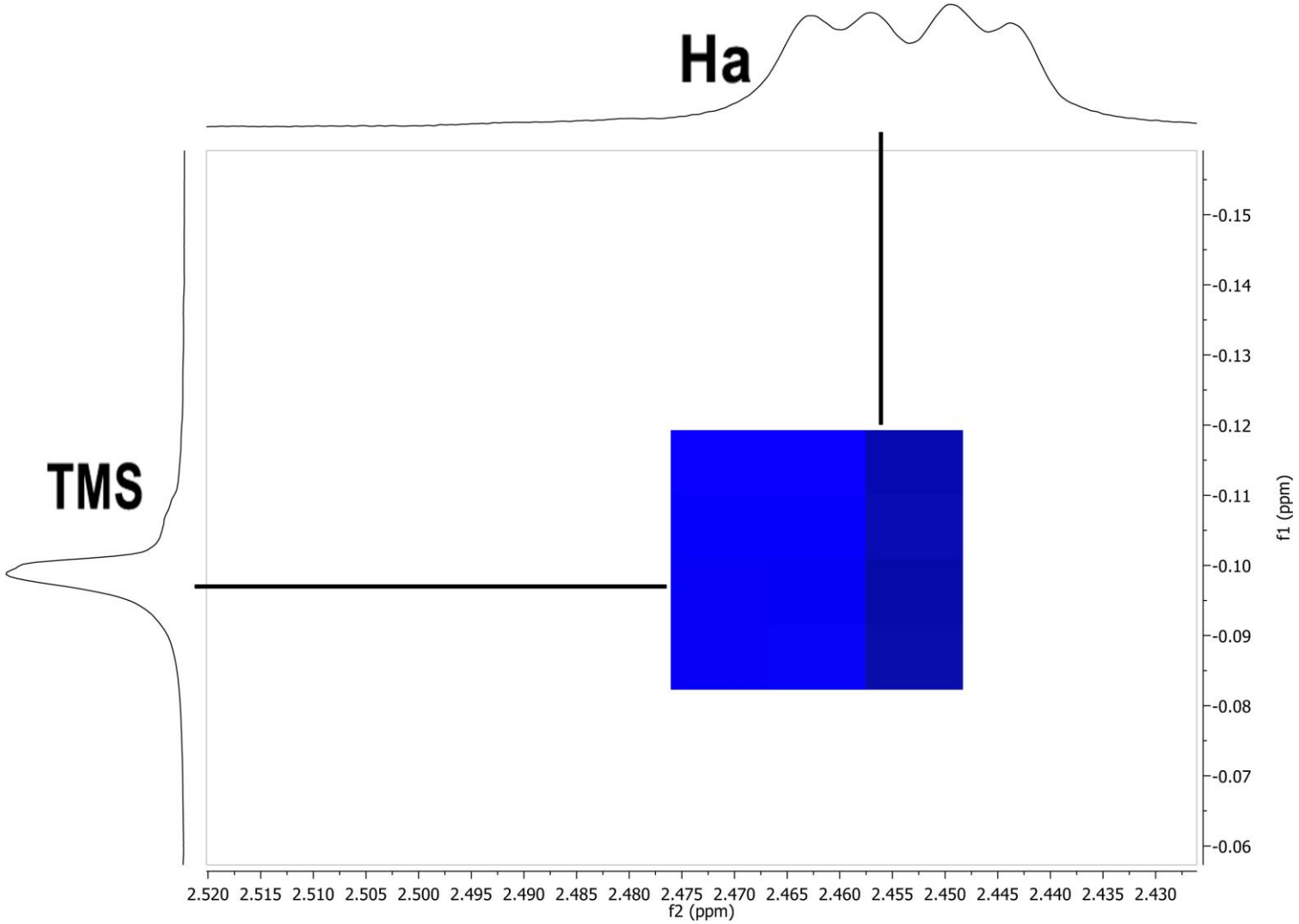

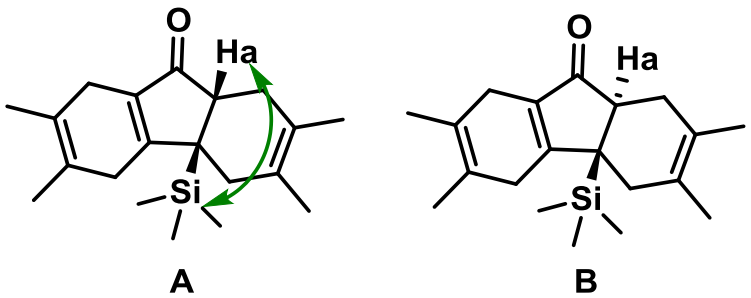

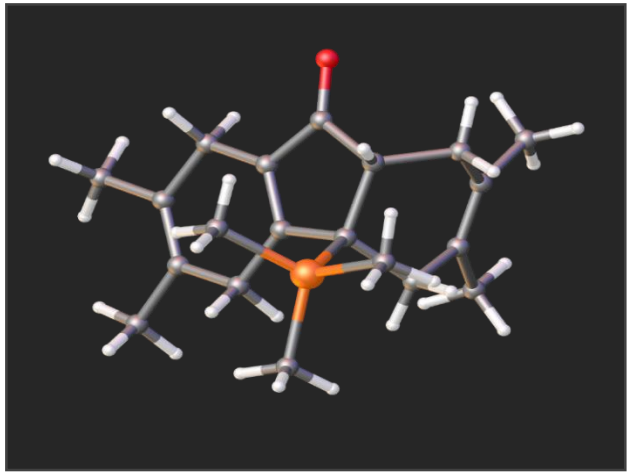

Major Isomer

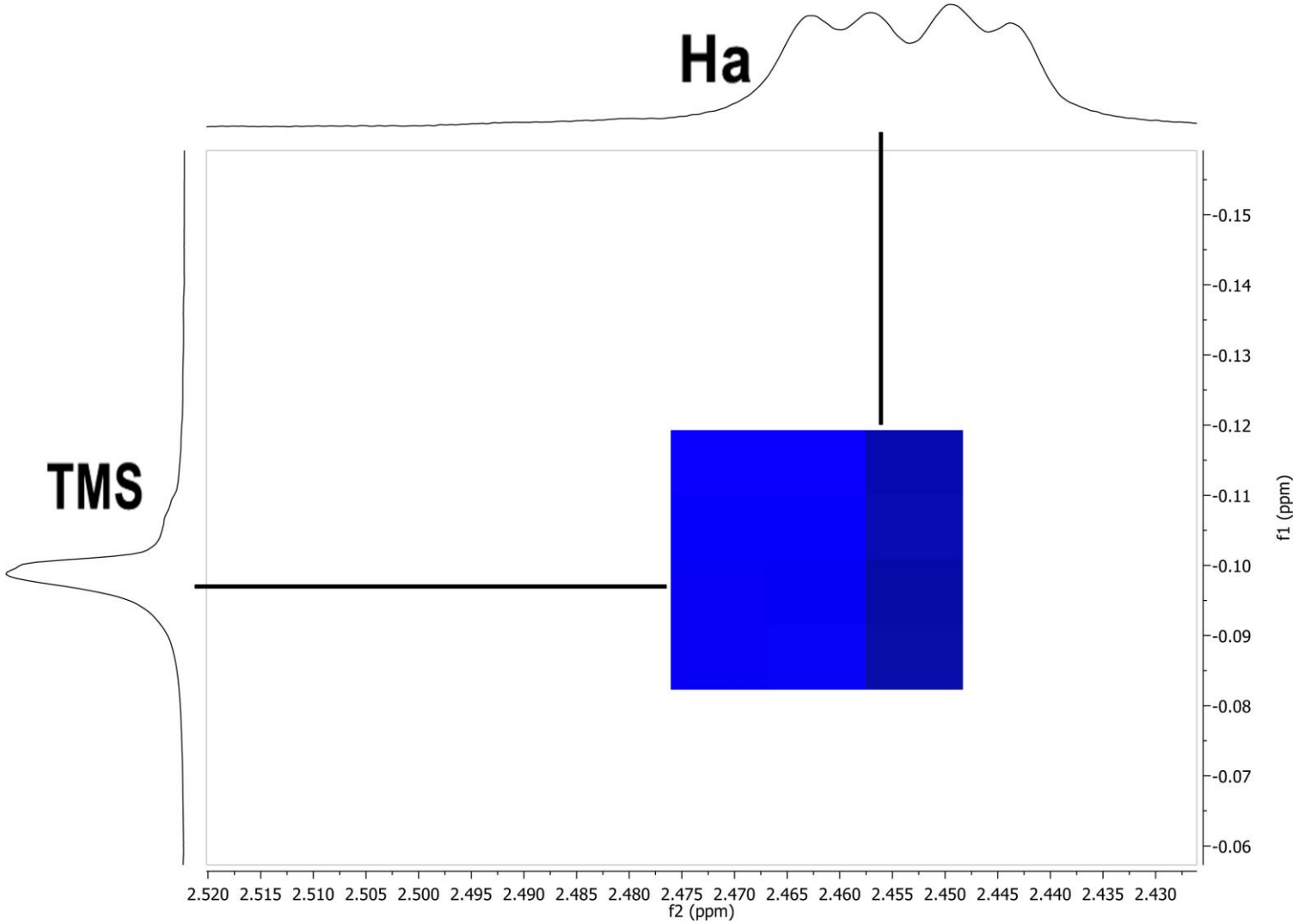

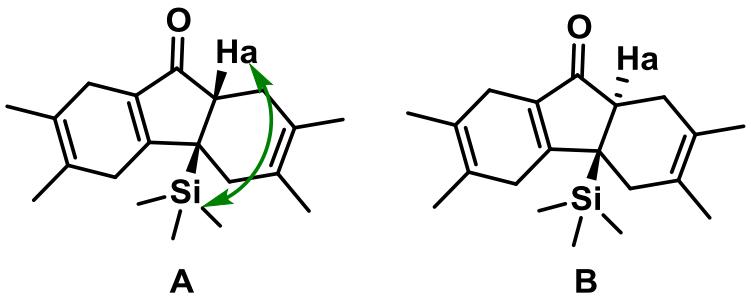

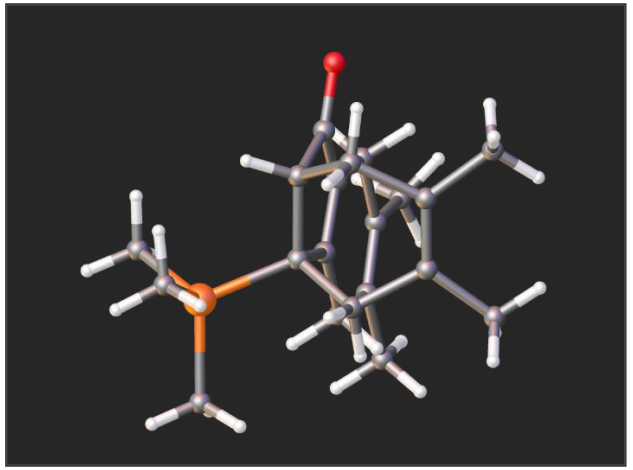

Symmetric Examples

- **Silane Derivatives**
  - **Demonstrate method versatility**
  - **Consistent stereochemical and regiochemical outcome**
- **Non-silane derivatives**
  - **Methyl and phenyl substituents**
  - **Formation of vicinal quaternary carbons**

TMS = 
Me = 
Ph = 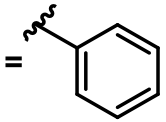

Diynone	Product	Yield (%)	Isomeric Ratio
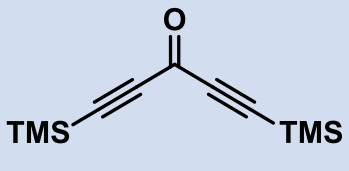	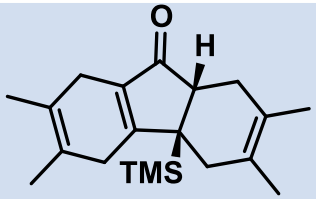	78	21:1
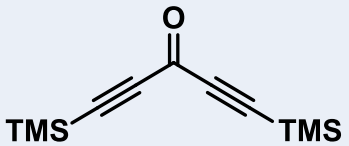	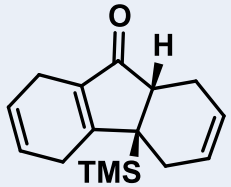	65	>99:1
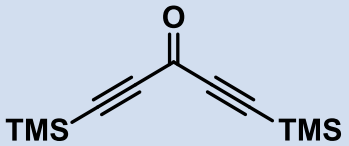	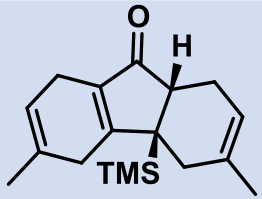	54	7:1.4:1:1
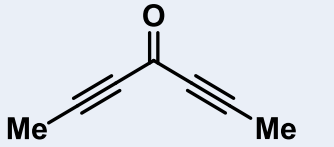	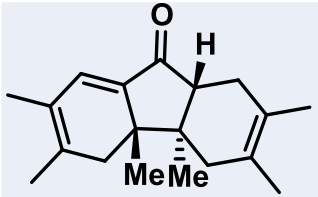	35	15:1
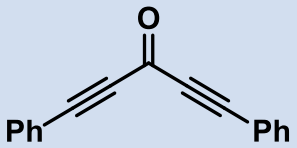	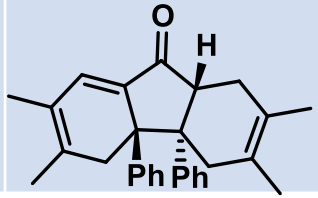	27	>20:1

R. A. Carmichael, W. A. Chalifoux (February 2016) Submitted to Angewandte Chemie International

Asymmetric Examples

- **Silane group always eliminates to give double bond**

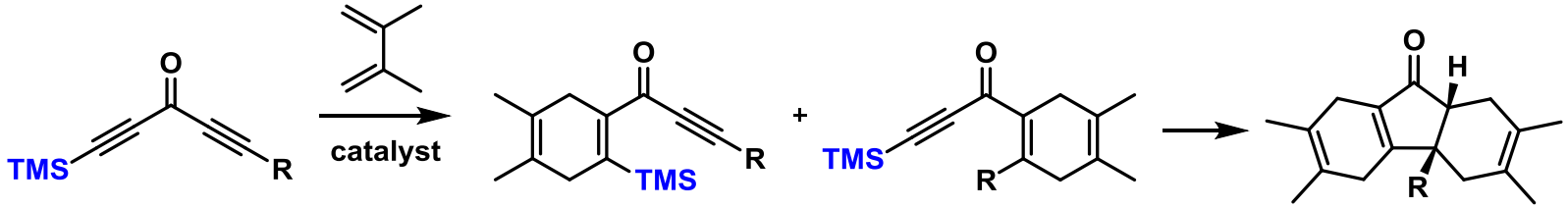

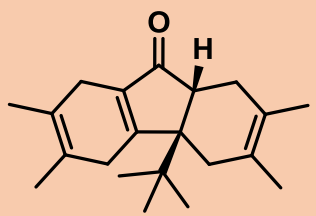	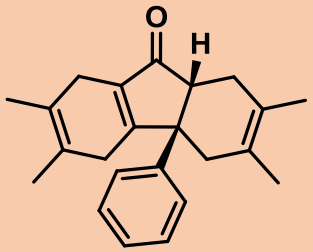	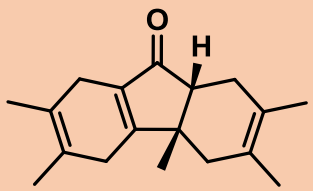	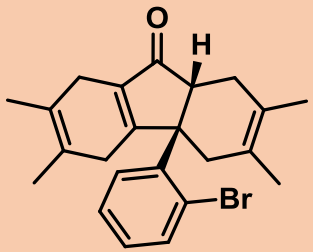	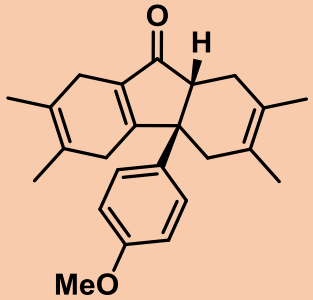
43%	35%	31%	46%	26%

Asymmetric: Multi-diene

- **Control product formation at low temperatures**

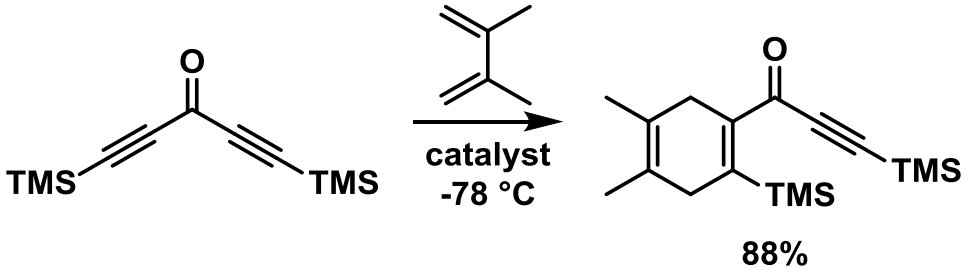

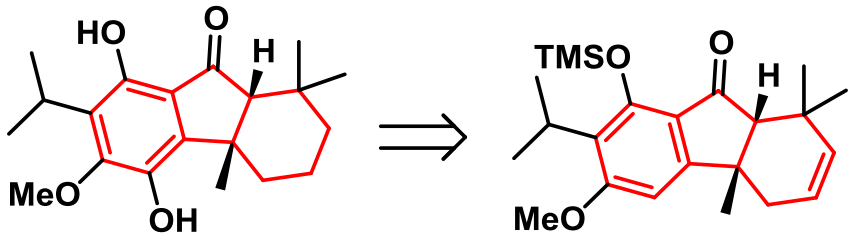

taiwaniaquinol B

[6,5,6] skeleton

- **Apply low temperature conditions to asymmetric reactions**
  - **Silane substituted alkyne undergoes Diels-Alder cyclization first**

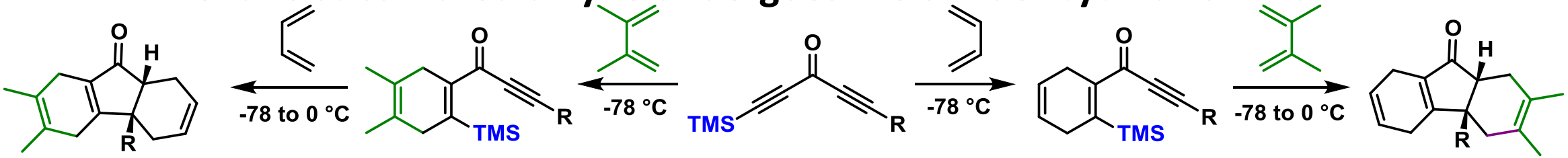

Fillion, E; Fishlock, D. *J. Am. Chem. Soc.* **2005**, *127*, 13144-13145

Future Endeavors

Optimize and complete asymmetric substrate scope

Develop enantioselective assay

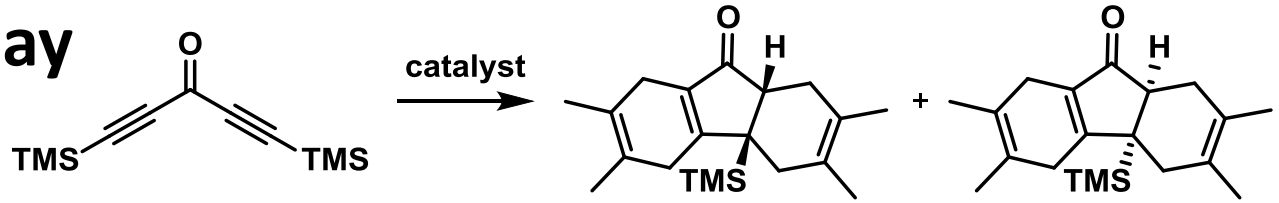

- **Apply method to the synthesis of an important target molecule**
  - **Work with collaborators to screen compounds for high priority viruses**

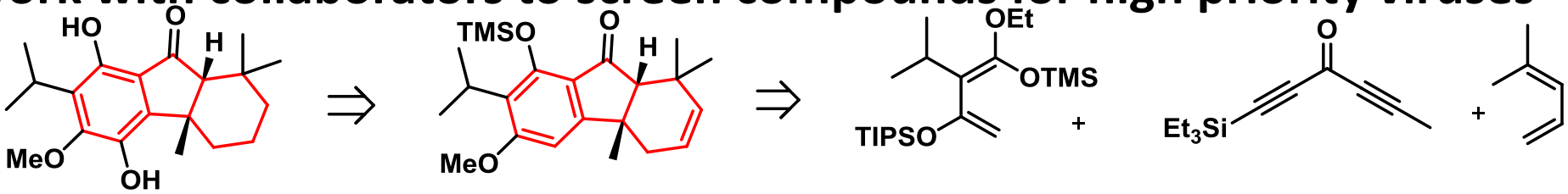

taiwaniaquinol B **[6,5,6] skeleton** **readily or commercially available starting materials**

Fillion, E; Fishlock, D. *J. Am. Chem. Soc.* **2005**, *127*, 13144-13145

Special Thanks to….

- **Dr. Wesley Chalifoux**
- **Chalifoux lab**
- **Nevada NASA Space Grant**
- **University of Nevada, Reno**

Questions?

Effect of Coherent Structures on Energetic Particle Intensity in the Solar Wind

Jeff Tessein
University of Delaware

Outline

- Background
- Instrumentation
- Results
- Analysis of Results

Background

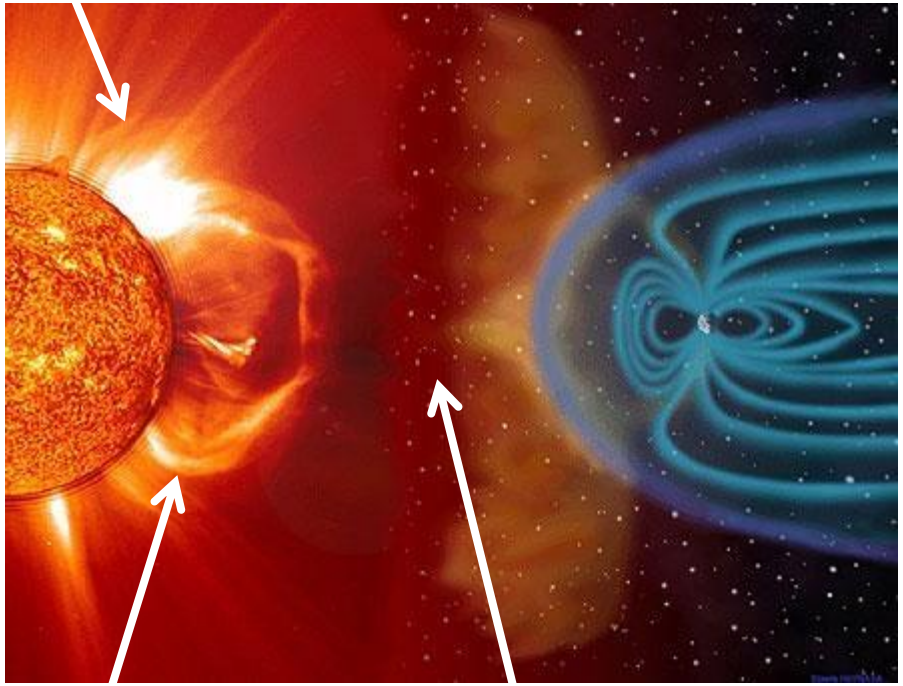

Space Weather

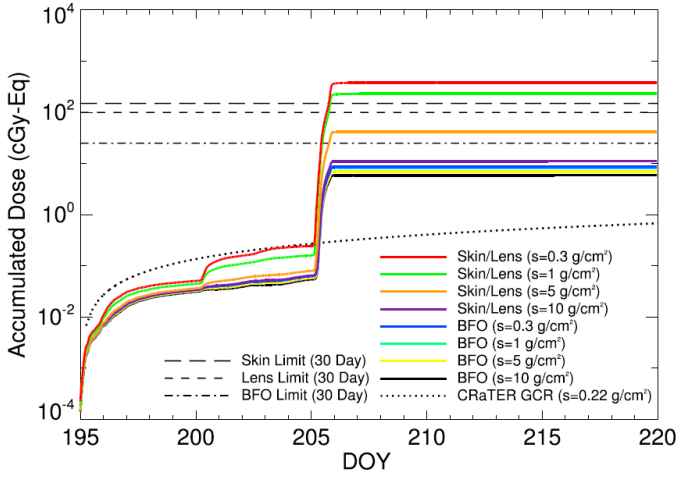

Joyce et al., Space Weather, 2015

- GPS guidance (tractors, ships)
- Racing pigeons

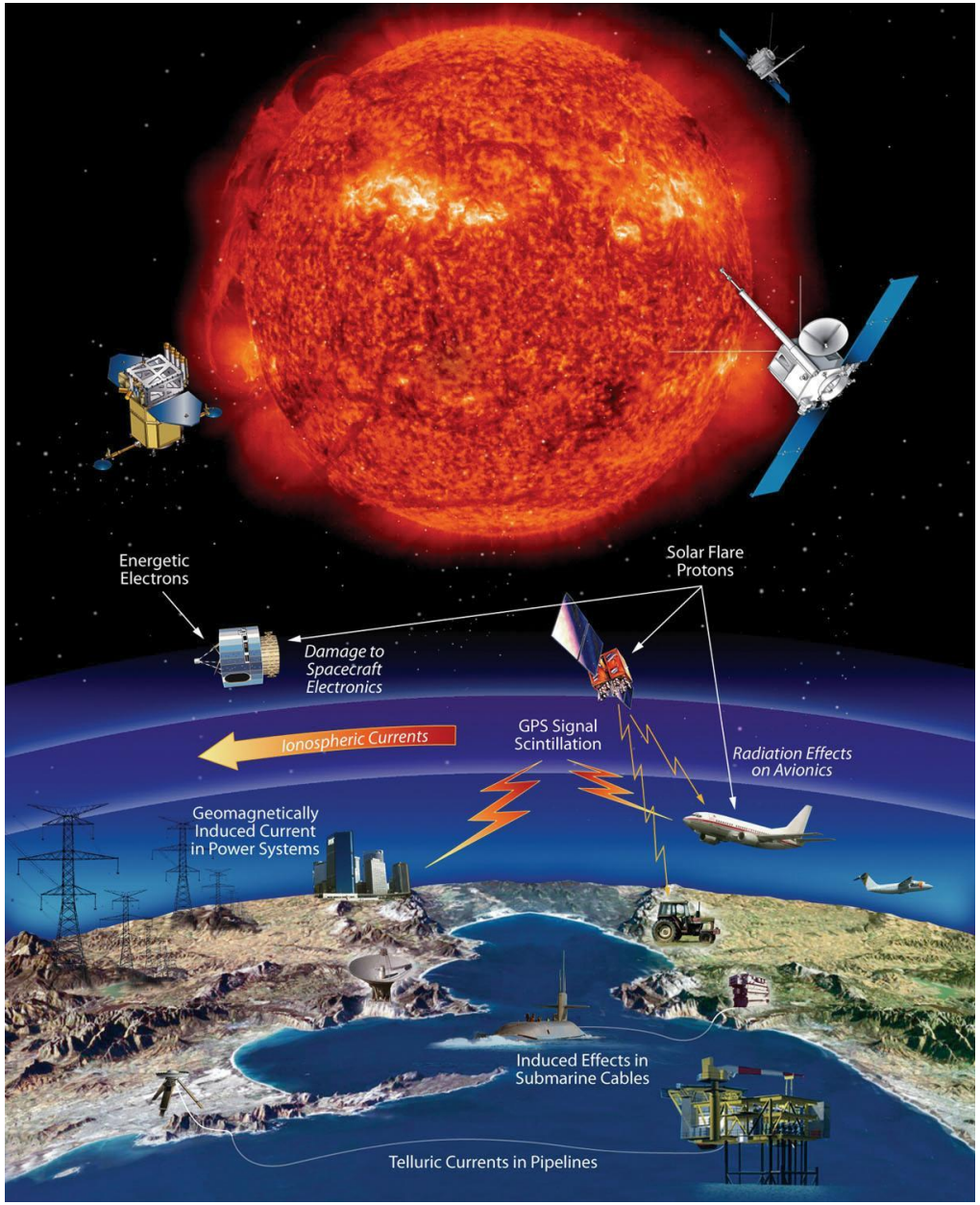

Image credit: NASA

Discontinuities

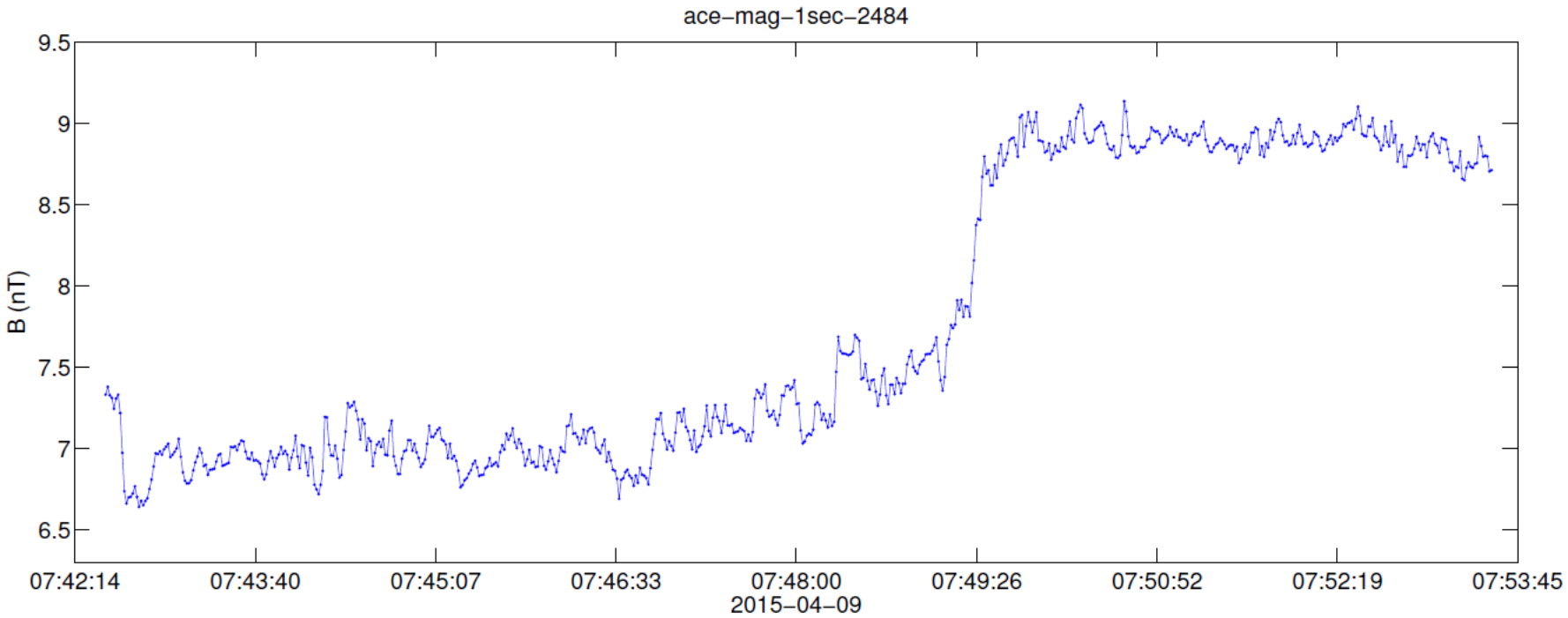

A change in the magnitude and/or direction of the fields.

Solar Energetic Particles (SEP)

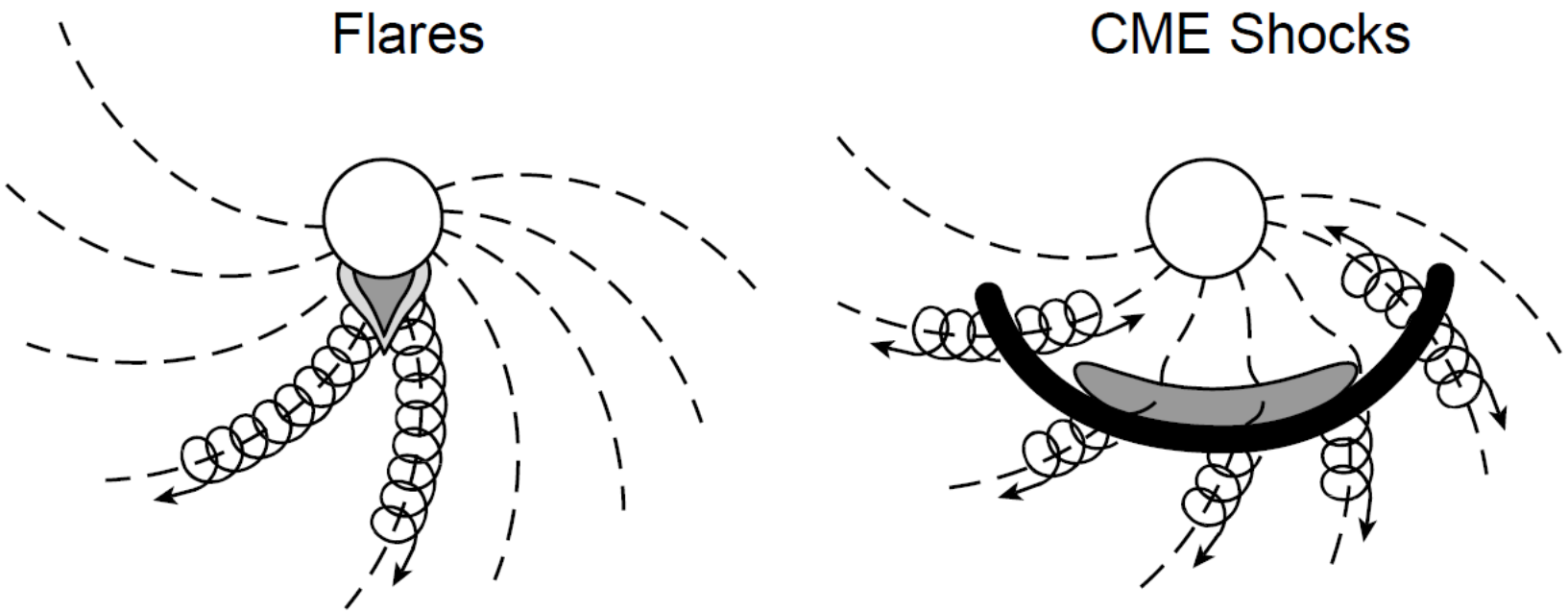

Classical picture since 1990s: two main mechanisms

Reames, SSR, 1999

PVI

- Used to locate discontinuities
- Useful for comparison with simulation

PVI: $\Im^{(2)} = \frac{|\Delta \mathbf{B}|^2}{\Sigma^2}$ $\quad \Sigma^2 = \langle |\Delta \mathbf{B}|^2 \rangle$

(Greco et al. 2008)

$\Delta \mathbf{B}$ is increment $\mathbf{B}(t+\tau) - \mathbf{B}(t)$

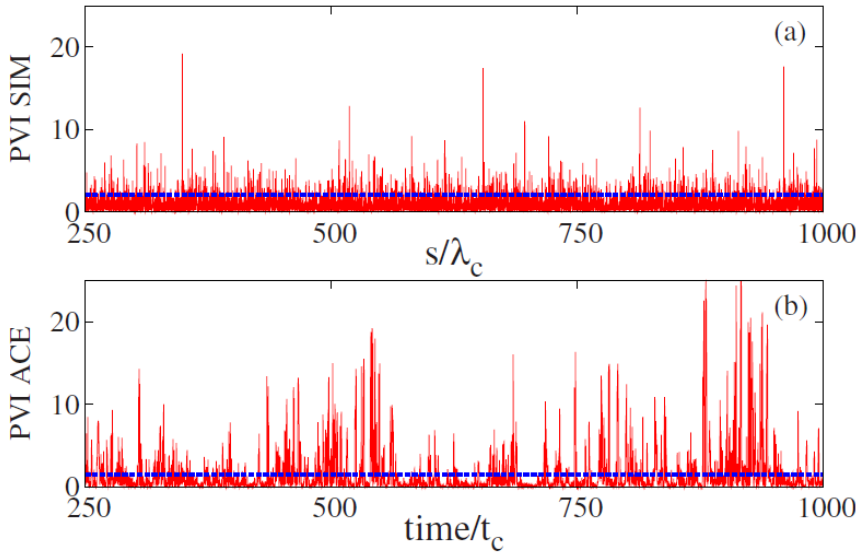

Greco et al. PRE 2009

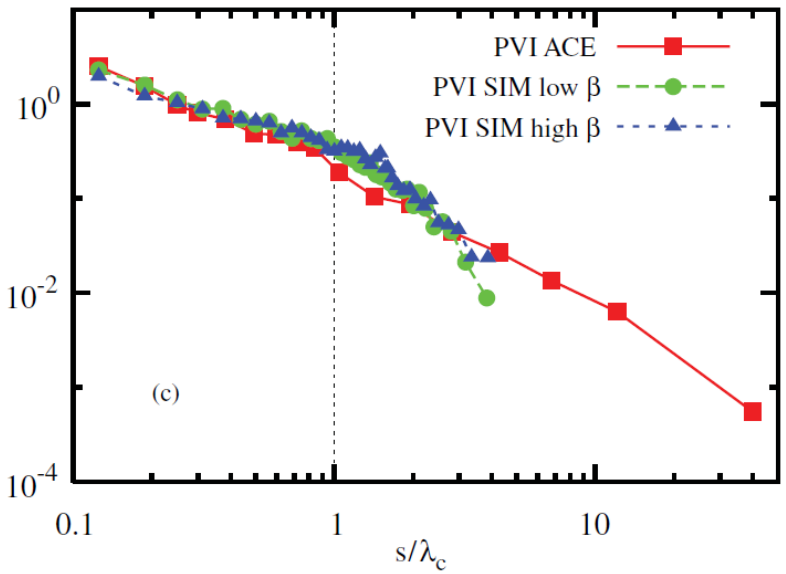

Greco et al. ApJ 2009

Instrumentation

Advanced Composition Explorer (1997)

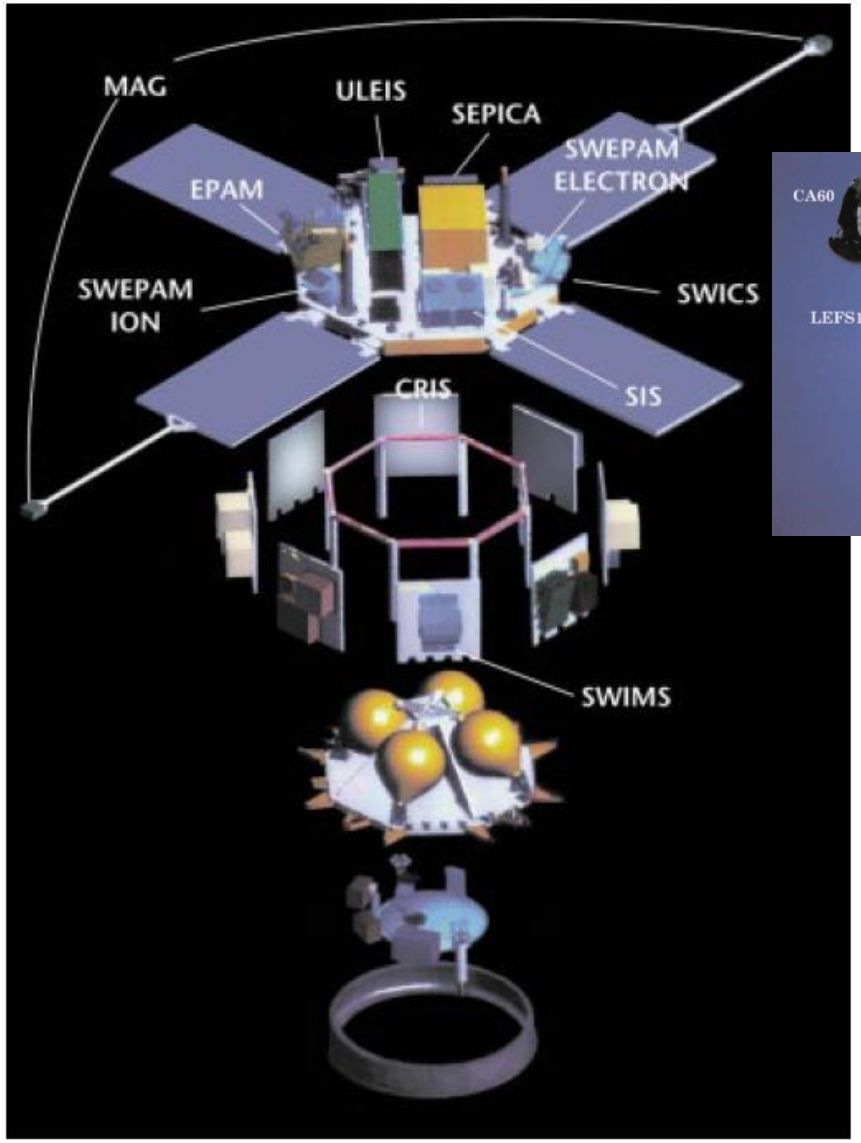

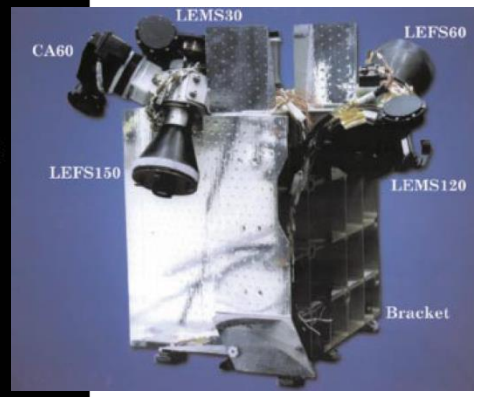

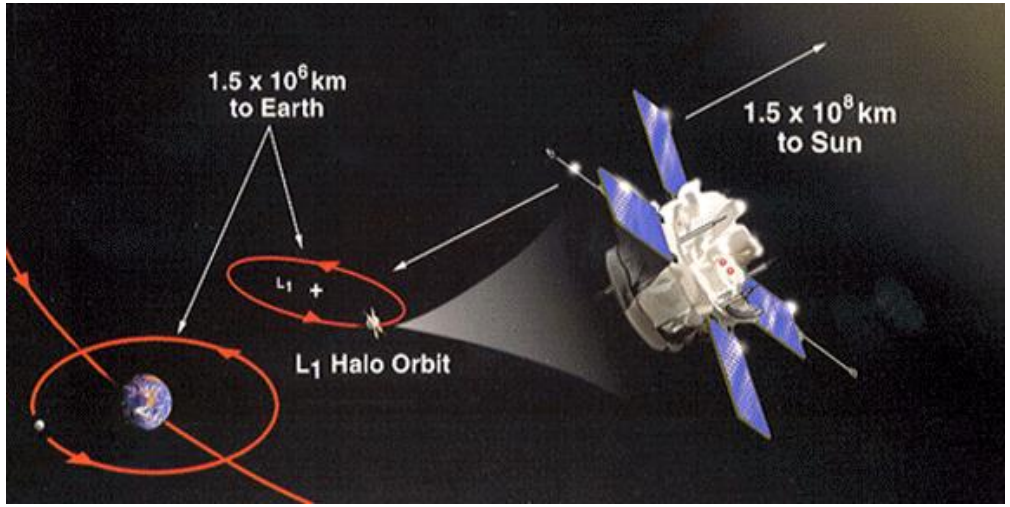

Stone et al., SSR, 1998, Gold et al., SSR, 1998

Data Analysis

- Conditional statistics, superposed epoch analysis
- Sum over 8 energy channels of ACE/EPAM/LEMS
- ACE MAG/SWEPAM reduced to 5 minute temporal resolution for comparison with EPAM
- **How do magnetic field discontinuities affect energetic particle intensity?**

Table 1
Summary of the data used.

Instrument	Measurement	Energy Range	Cadence	Time Interval[a]
ACE/EPAM/LEMS30	Ion Flux	0.046-4.7 MeV	5 minutes	1998-23 to 2001-050
ACE/EPAM/LEMS120	Ion Flux	0.047-4.78 MeV	5 minutes	1998-23 to 2010-258
ACE/SWEPAM & MAG	Plasma Parameters & Magnetic Field	0.26-36 keV	64 seconds	1998-23 to 2010-258
ACE/MAG	Magnetic Field	N/A	16 seconds	1998-23 to 2010-258

[a]Time format is (year)-(day of year)

Results

Stronger Discontinuities Associated with Higher Average Energetic Particle Flux

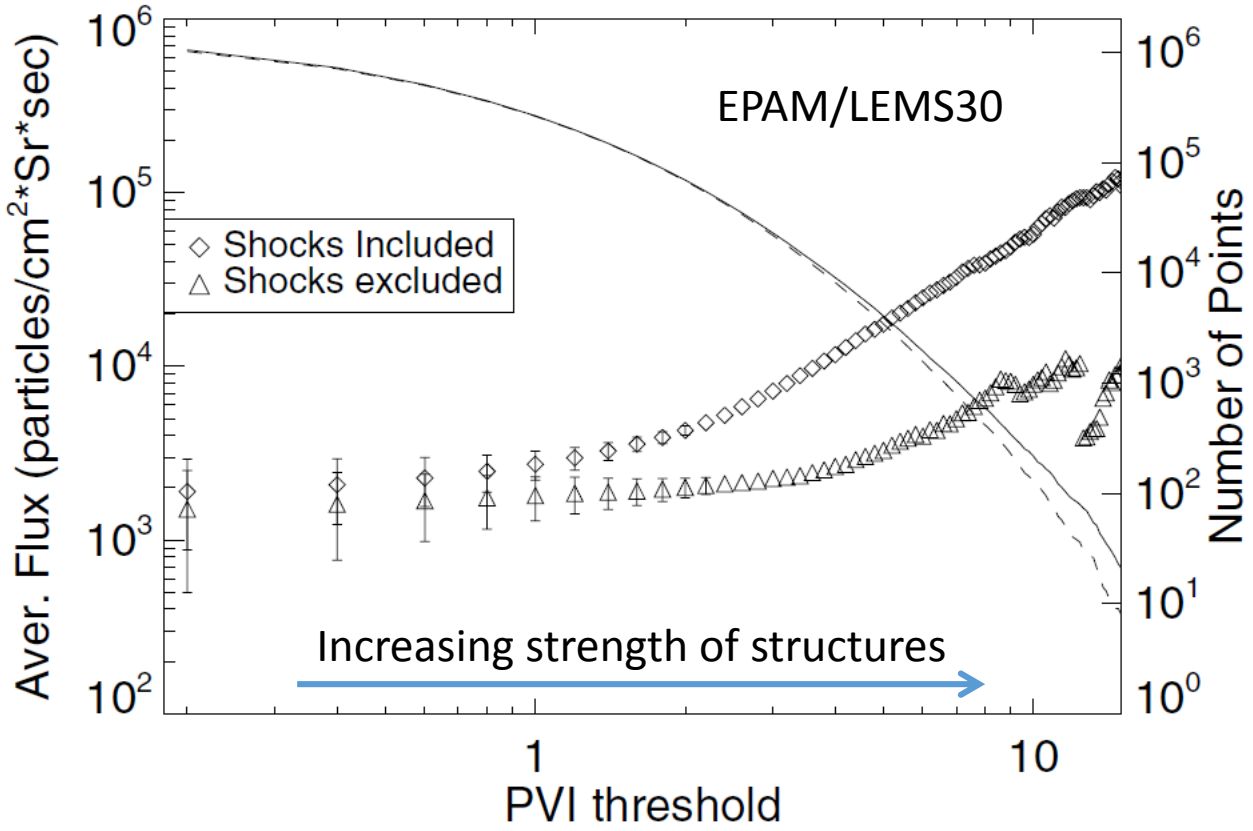

Shock exclusion: 12 hours of data removed on either side of the shock

Tessein et al., ApJL, 2013

Average Energetic Particle Flux Peaks Near Discontinuities

Shock neighborhoods included

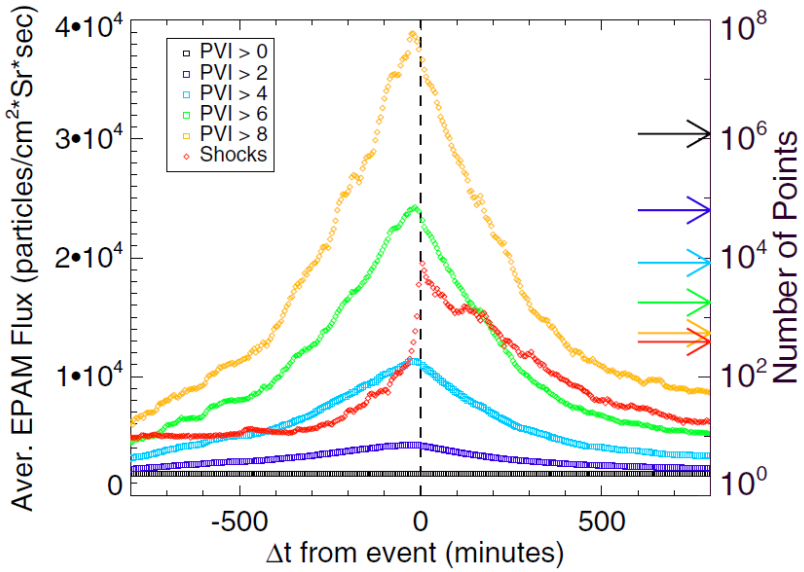

Superposed Epoch Analysis, 322 Shocks from ACE list

Shock neighborhoods excluded

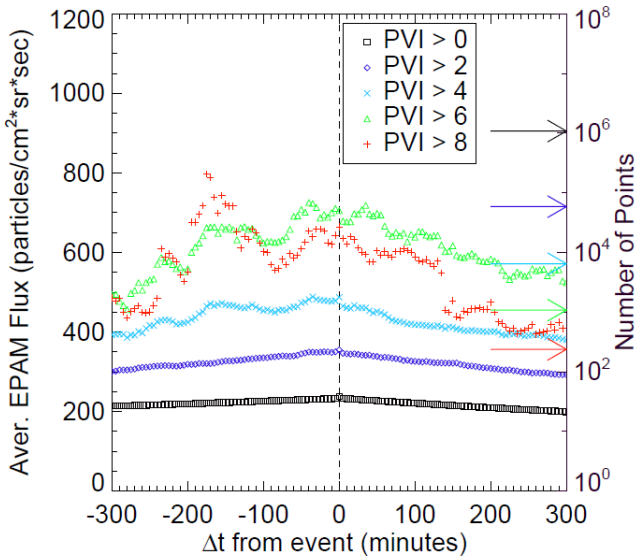

PVI > 8 trace is messy. Different mechanism or poorer statistics?

Tessein et al., ApJL, 2013

Tessein et al., ApJ, 2015

Analysis of Results

What leads to these results?

1. Presence of shocks not in the list
2. Extended shock acceleration events
3. Edge events

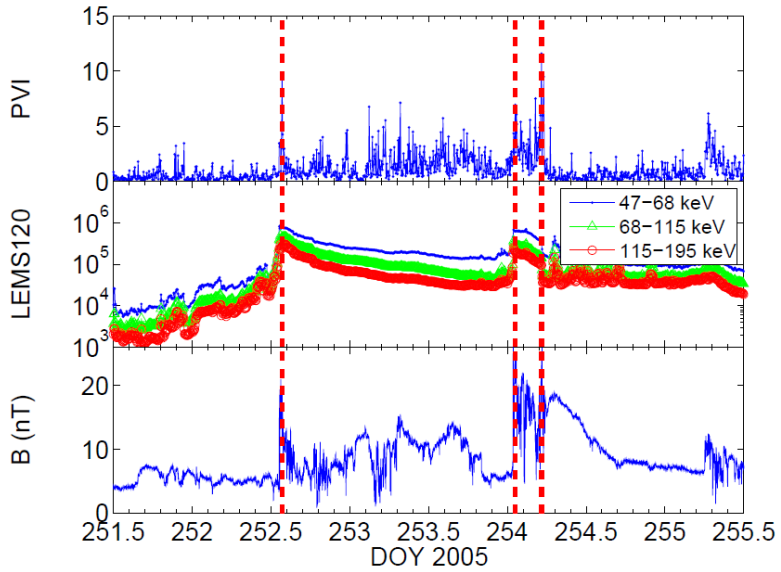

Tessein et al., ApJ, 2015

What leads to these results?

1. ~~Presence of shocks not in the list~~
2. Extended shock acceleration events – Will not produce a peak
3. Edge events – Possible flux tube boundary or local acceleration site

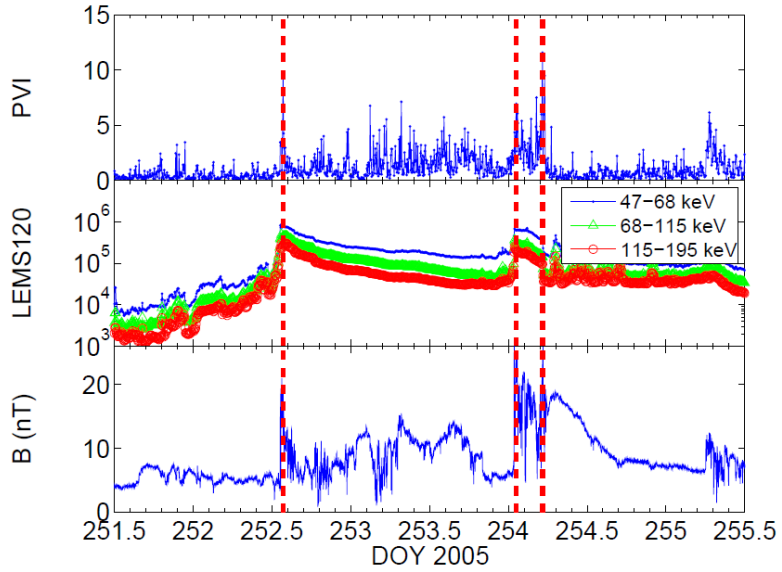

Tessein et al., ApJ, 2015

Edge Events

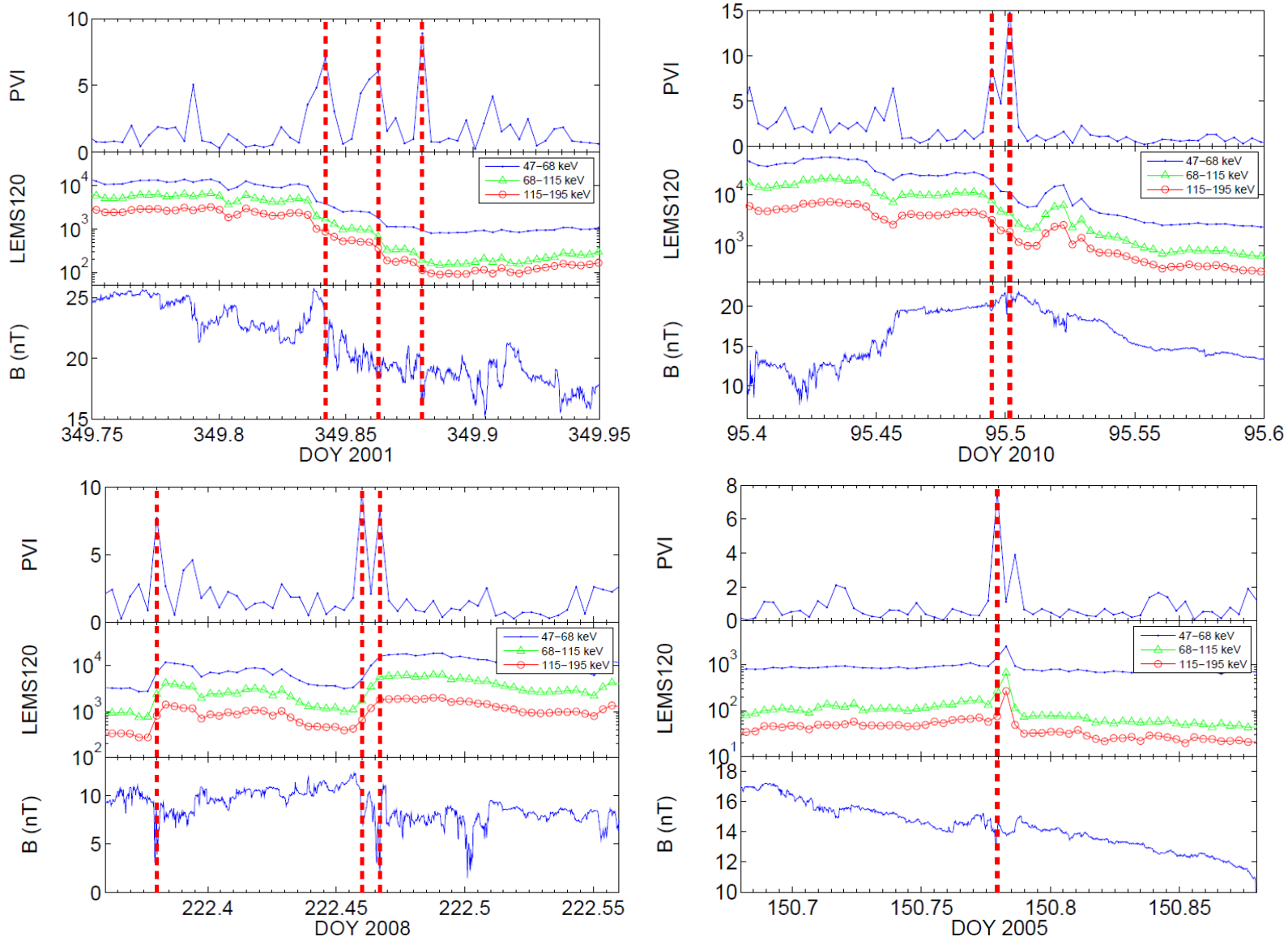

Tessein et al., ApJ, 2015

Possible Flux Tube Boundary

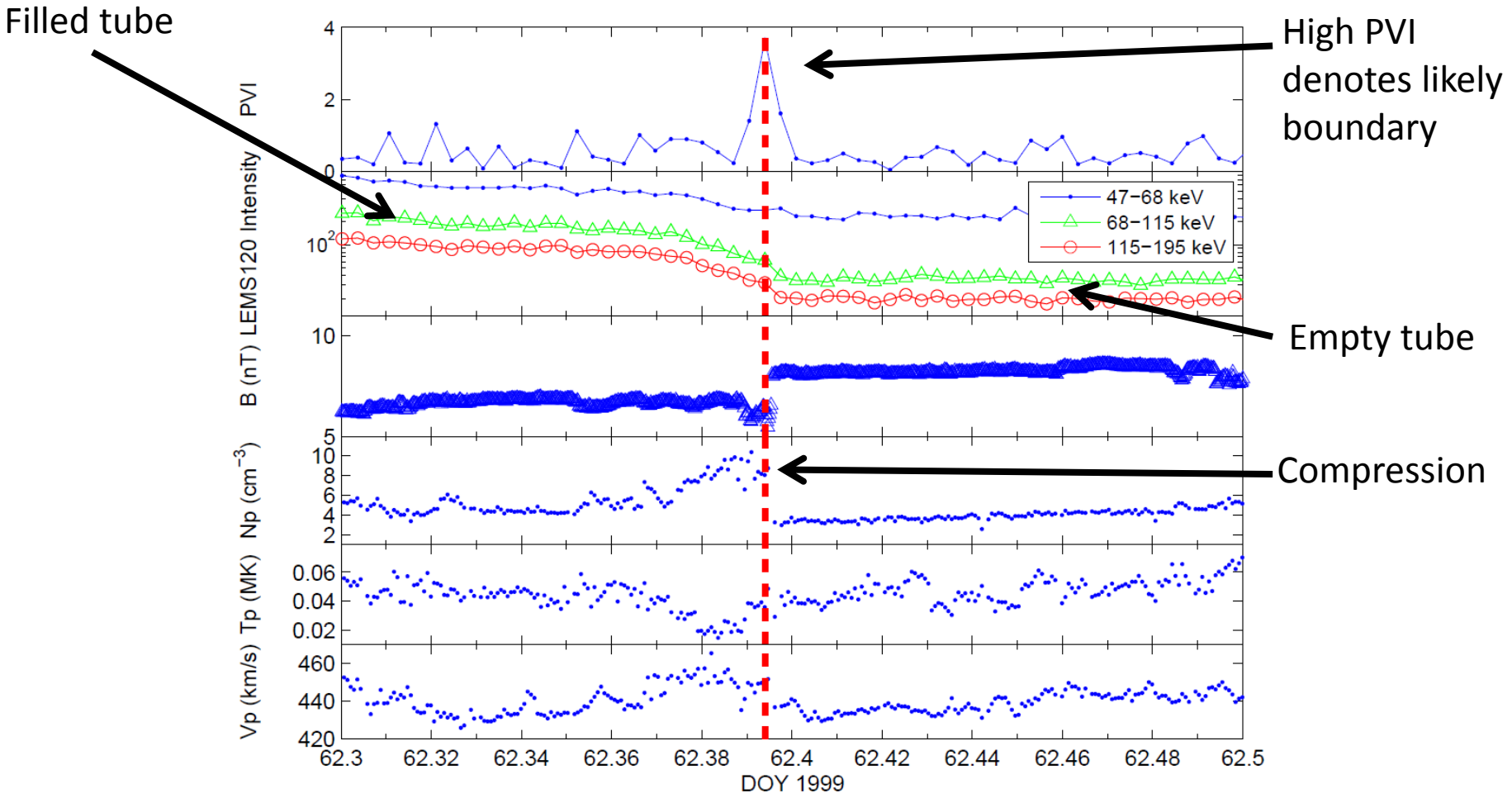

Tessein et al., ApJ, 2015

Conclusions

- Energetic particle flux associated with magnetic structures
- Structures are likely flux tube boundaries
- Local acceleration possible
- There are implications for shocked regions

Additional Slides

Intermittency

Matthaeus et al. 2015: The degree to which nonlinearly interacting fluctuations may be expected to give rise to structure in space and in time

Increment: $\delta v_r(\boldsymbol{x}) = \hat{\boldsymbol{r}} \cdot [\boldsymbol{v}(\boldsymbol{x}+\boldsymbol{r}) - \boldsymbol{v}(\boldsymbol{x})]$

Structure function: $S^{(p)}(r) = \langle \delta v_r^p \rangle$

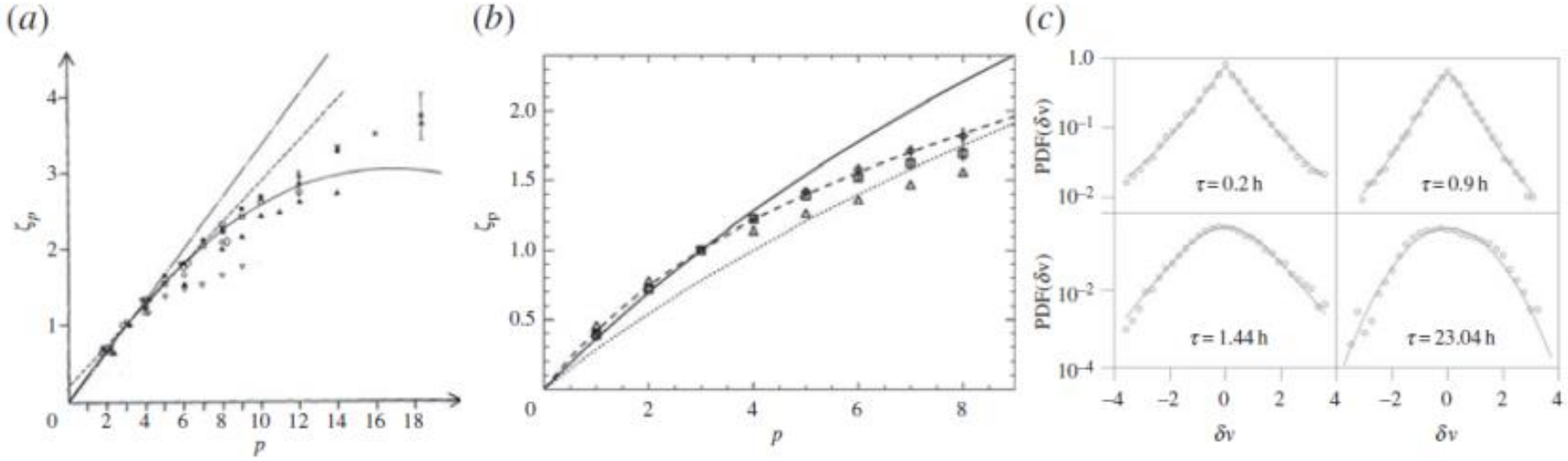

Anselmet et al., JFM, 1984; Biskamp & Müller, PoP, 2000; Sorriso-Valvo et al., GRL, 1999

Upstream Events in LEMS120

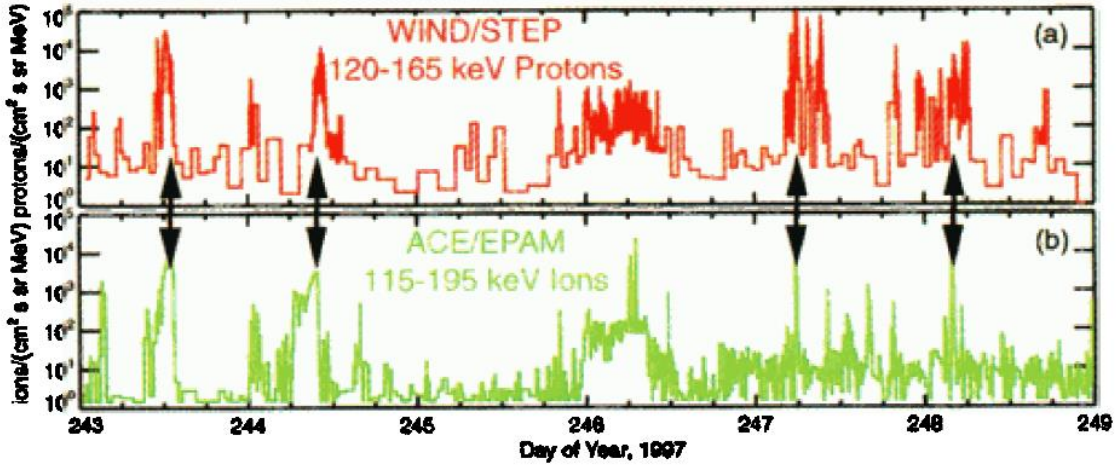

Haggerty et al., GRL, 1999

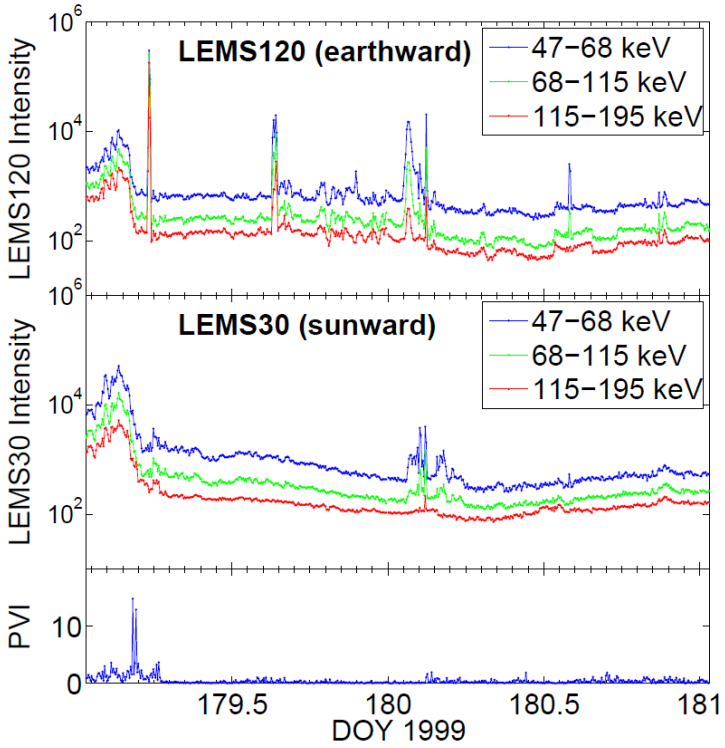

Tessein et al., ApJ, 2015

Coherent Structures- Heating

- Increased ion temperature in or near strong coherent structures

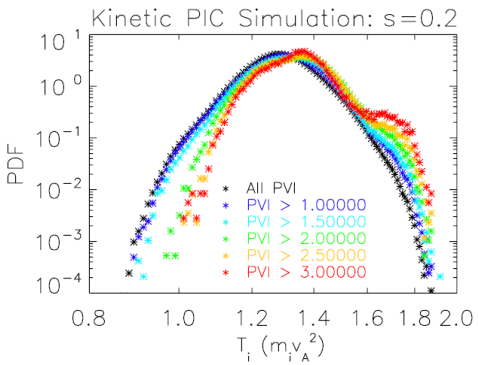

Wu et al., ApJL, 2013

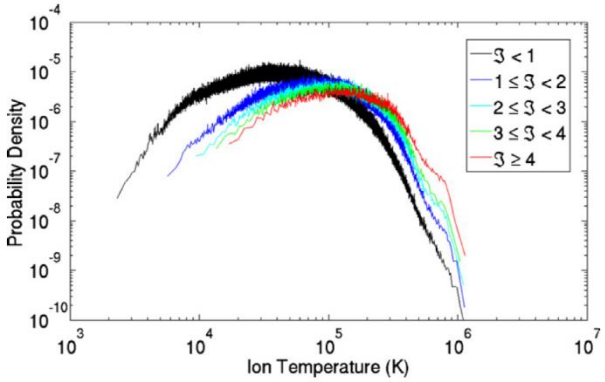

Osman et al., ApJL, 2011

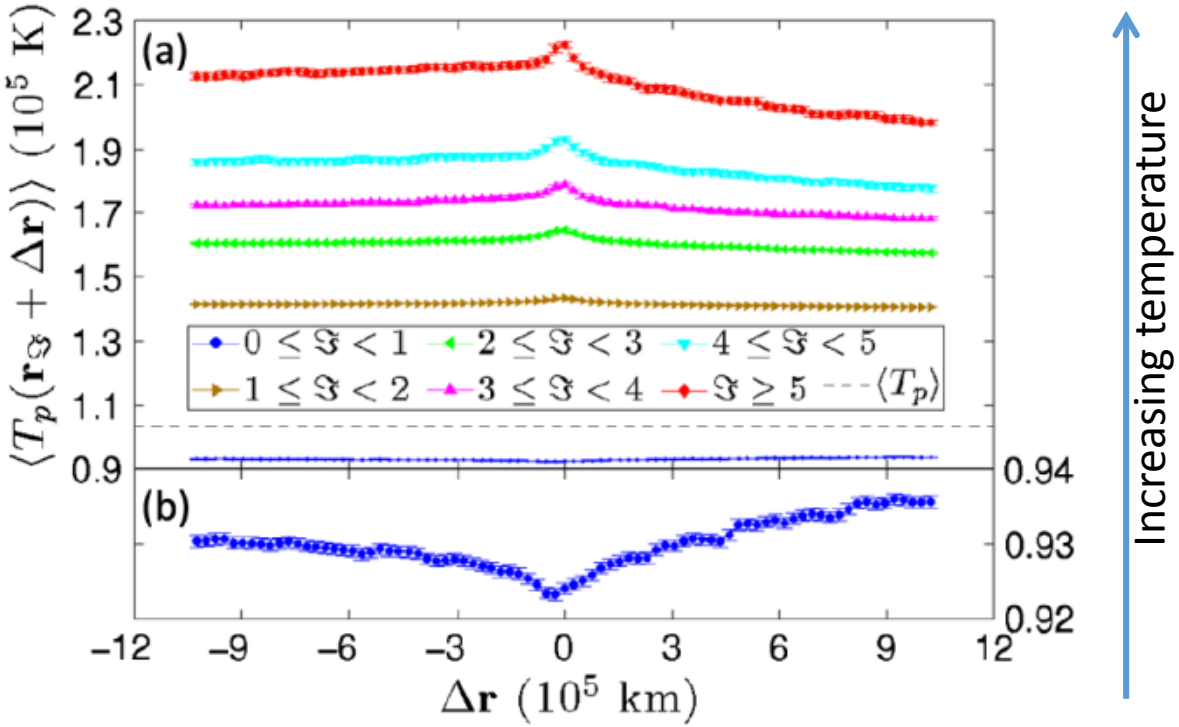

Osman et al., PRL, 2012

Increasing temperature

Problems with LEMS30

Elevated noise floor

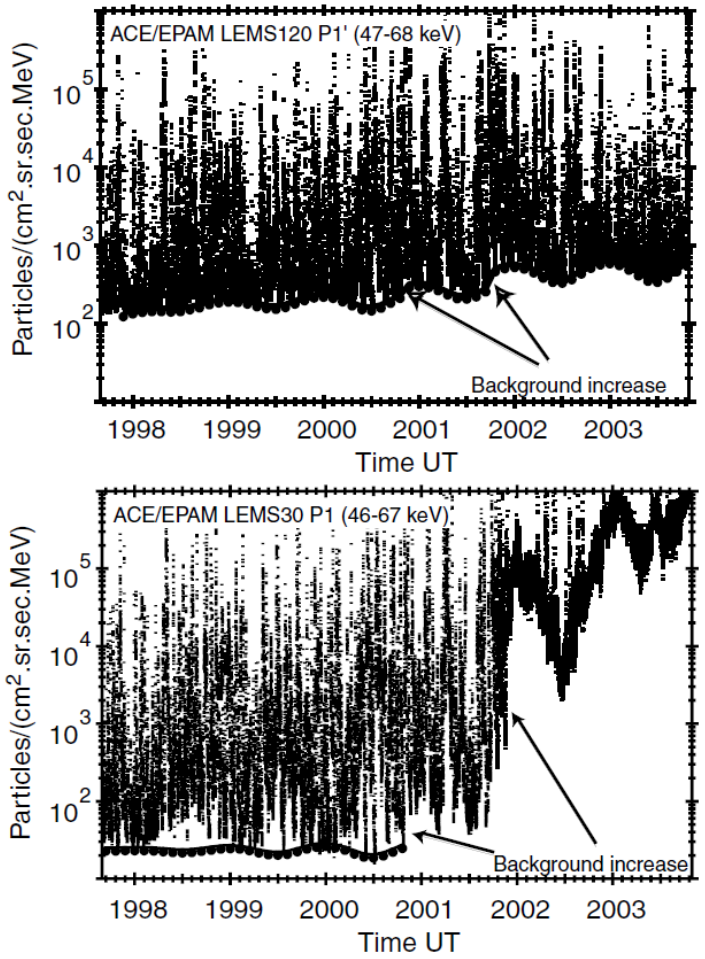

Haggerty et al., ASR, 2006

X-ray contamination

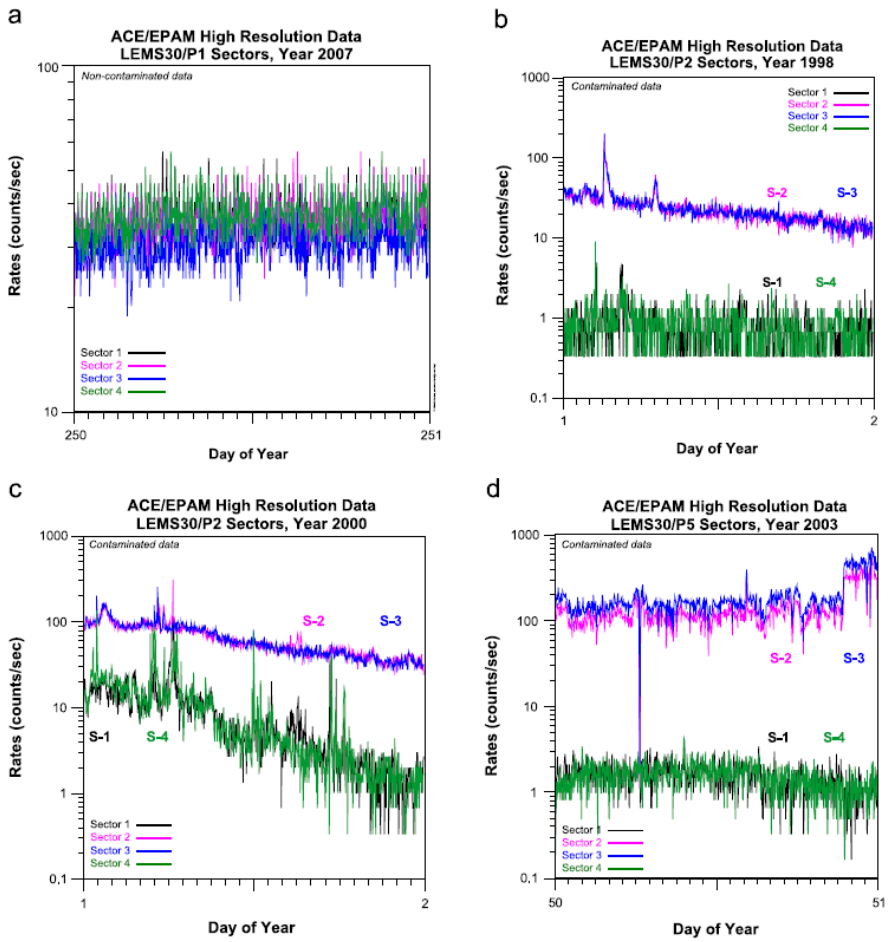

Marhavilas et al., P&SS, 2015

Shock Lists

- Not all shocks appear in the ACE list
- Use CfA Interplanetary Shock Database to complete list of shocks

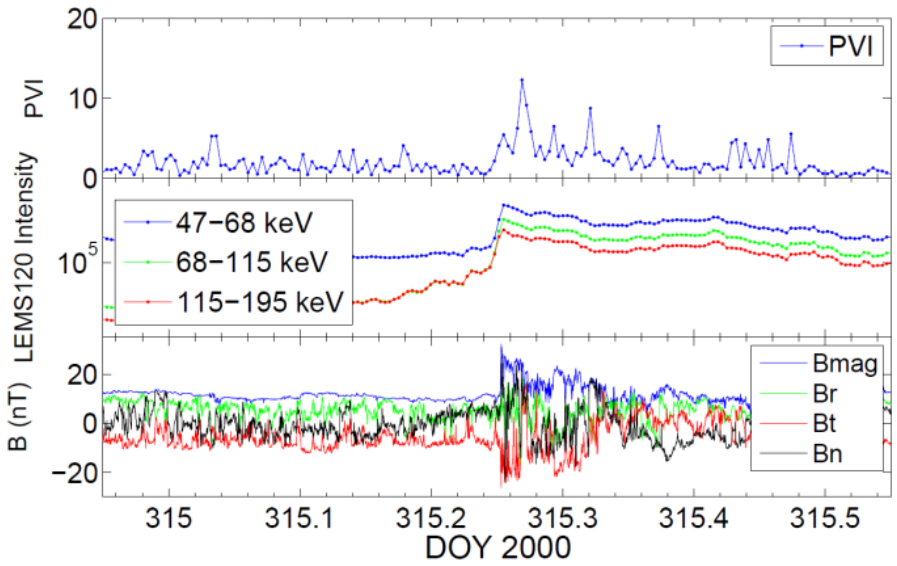

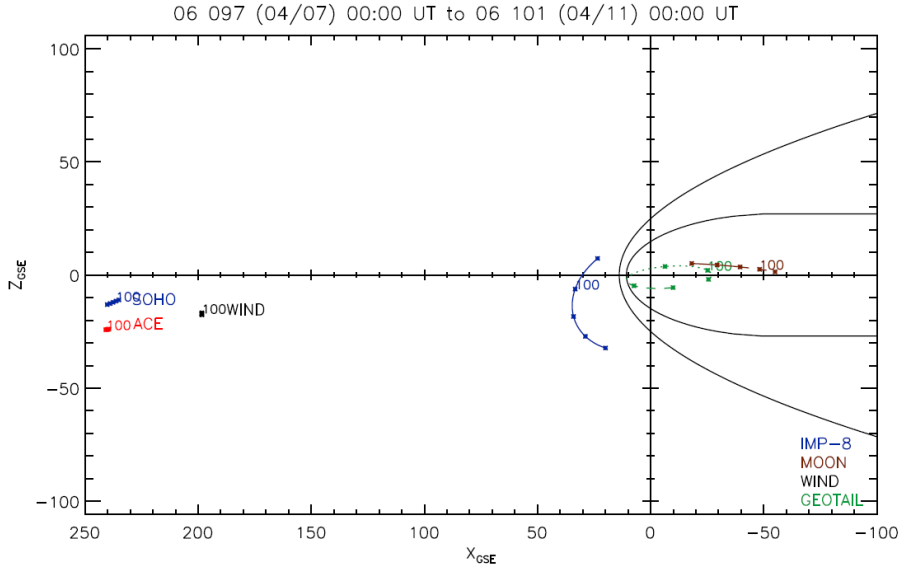

Flare Acceleration

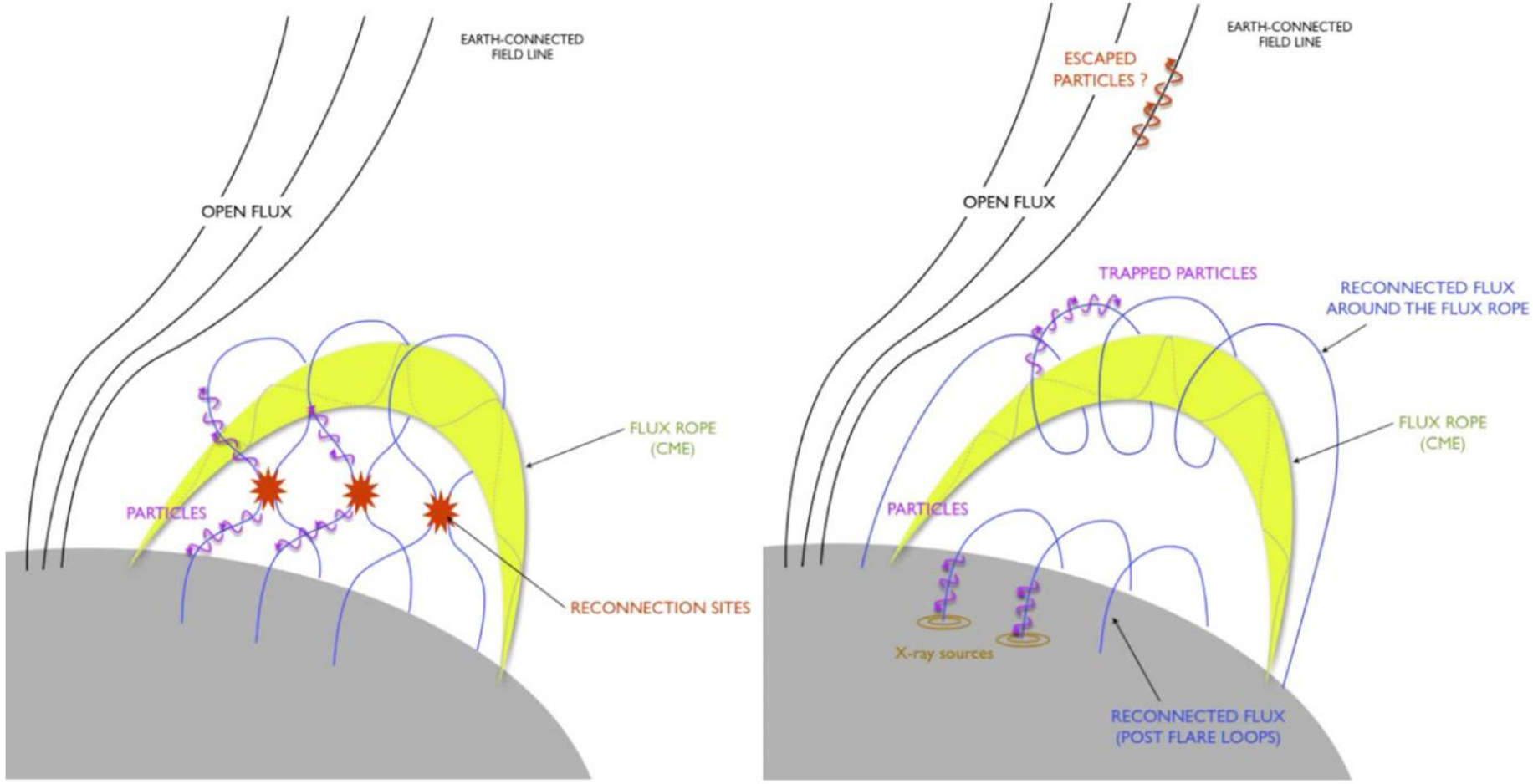

Masson et al., ApJ, 2013

Diffusive Shock Acceleration

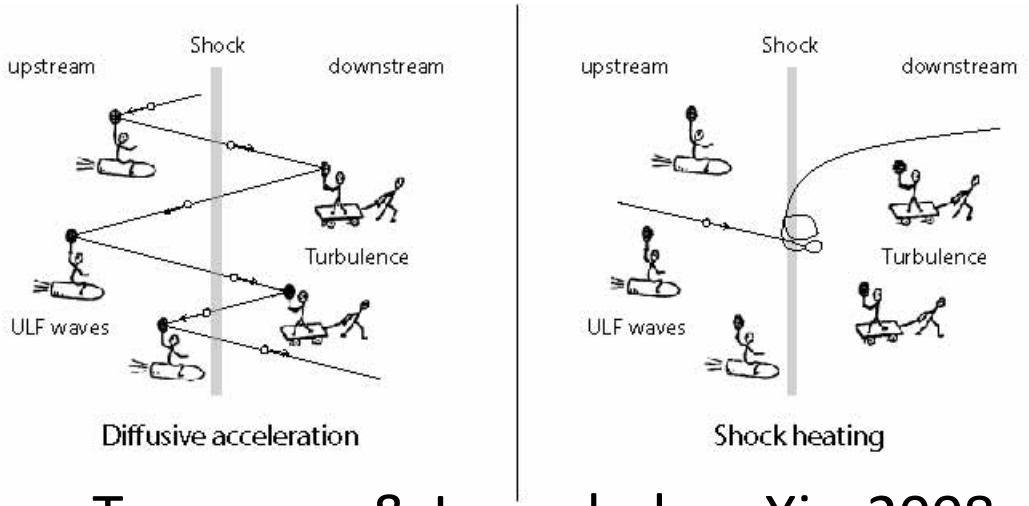

Treumann & Jaroschek, arXiv, 2008

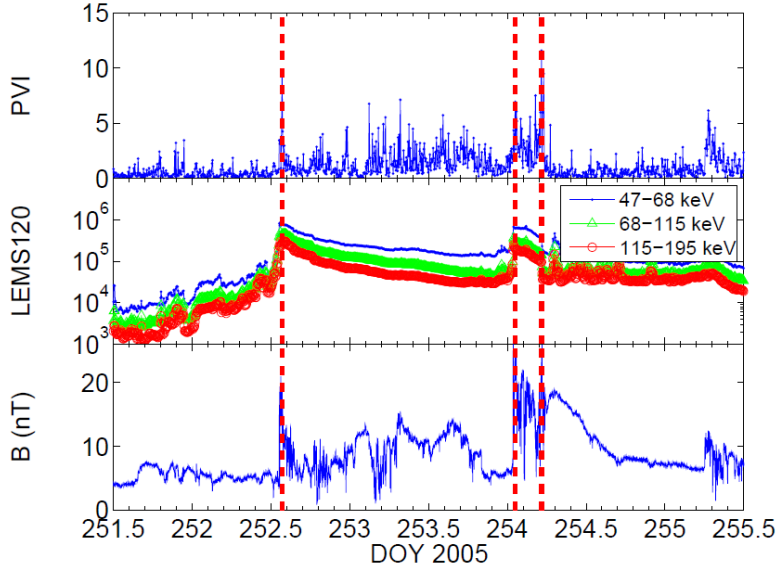

Tessein et al., ApJ, 2015

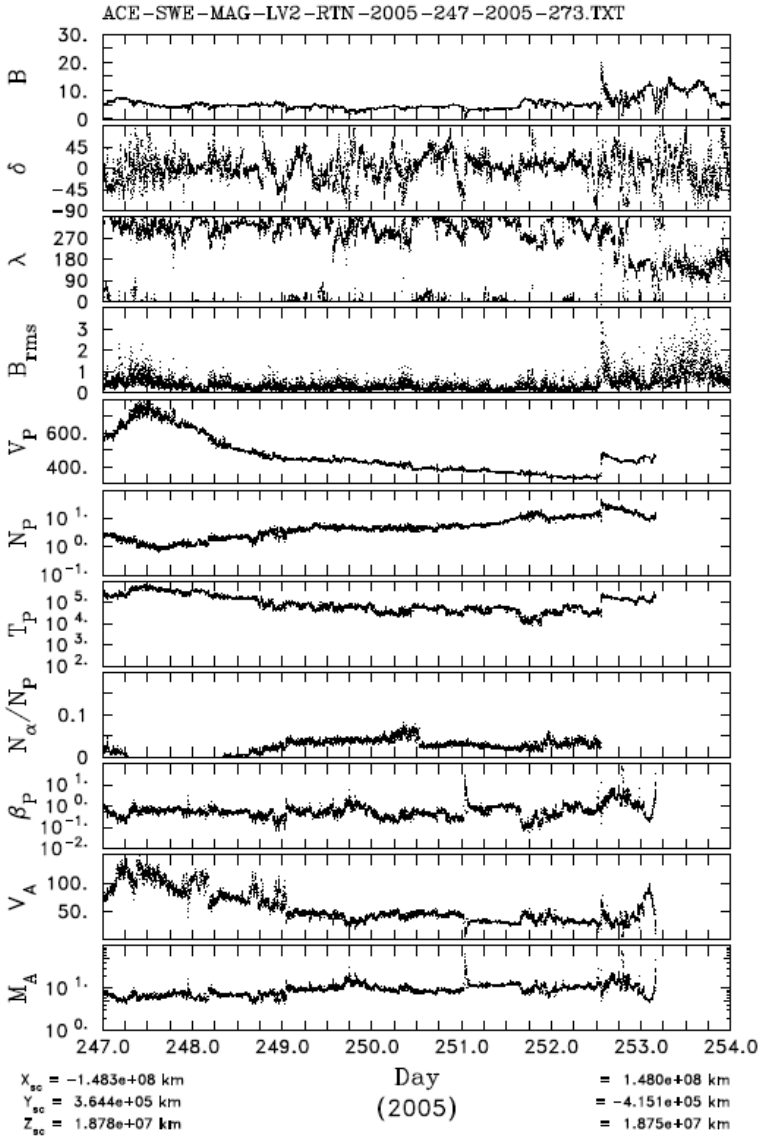

ACE Science Center

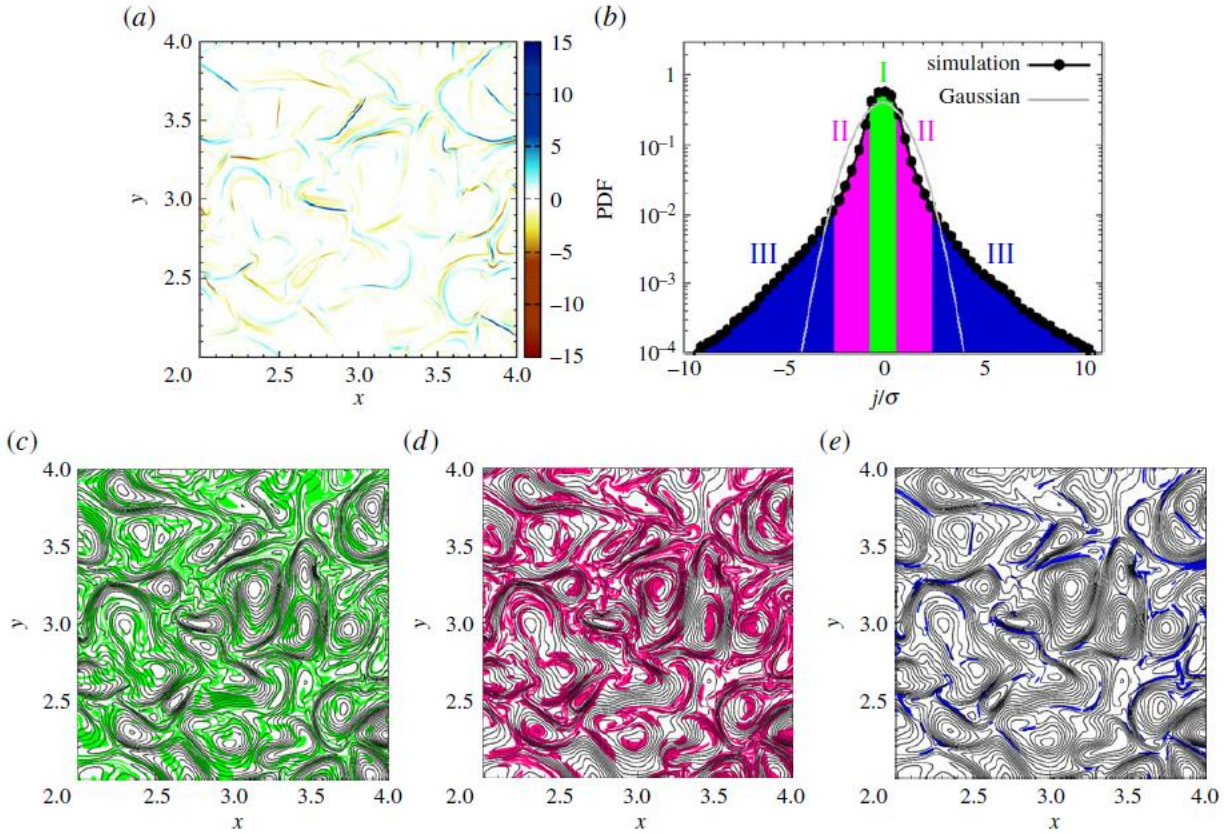

Strong current sheets are located between magnetic islands

Subedi et al., ApJ, 2014

Matthaeus et al., Phil. Trans. A., 2015

Kurtosis: $$\kappa(r) = \frac{\langle \delta v_r^4 \rangle}{\langle \delta v_r^2 \rangle^2}$$

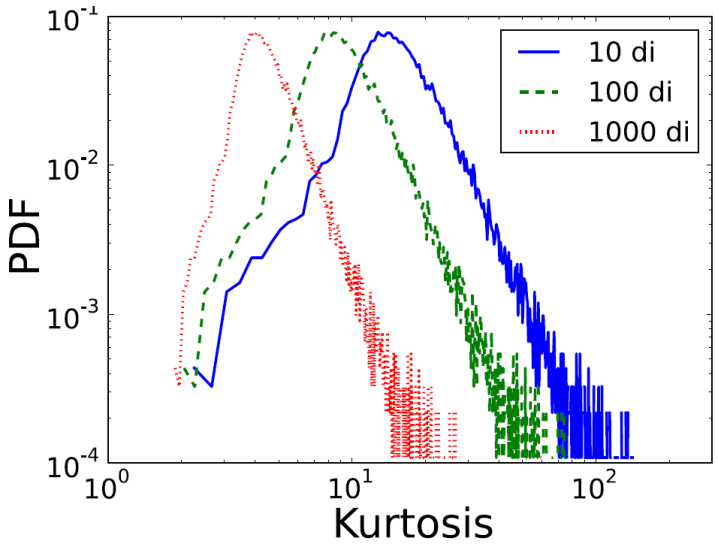

Signed Percent Difference

- Non-Gaussian distribution of energetic particle flux changes
- Statistical manifestation of thousands of PVI events showing small changes in energetic particle flux

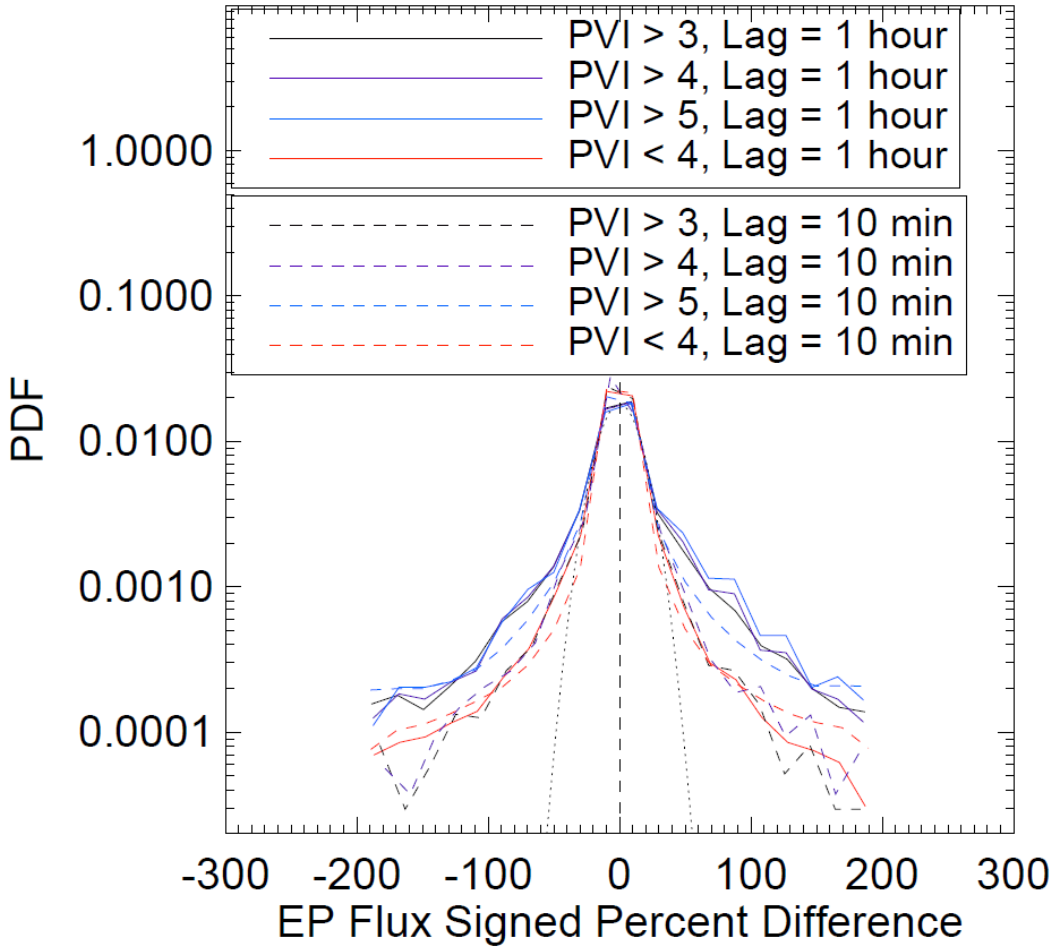

Tessein et al., ApJ, 2015

Weak shocks

Average energetic particle profiles for questionable shocks, strong shocks and PVI > 8 discontinuities (with shock neighborhoods included). There is no evidence of strong energetic particle flux increases associated with questionable shocks.

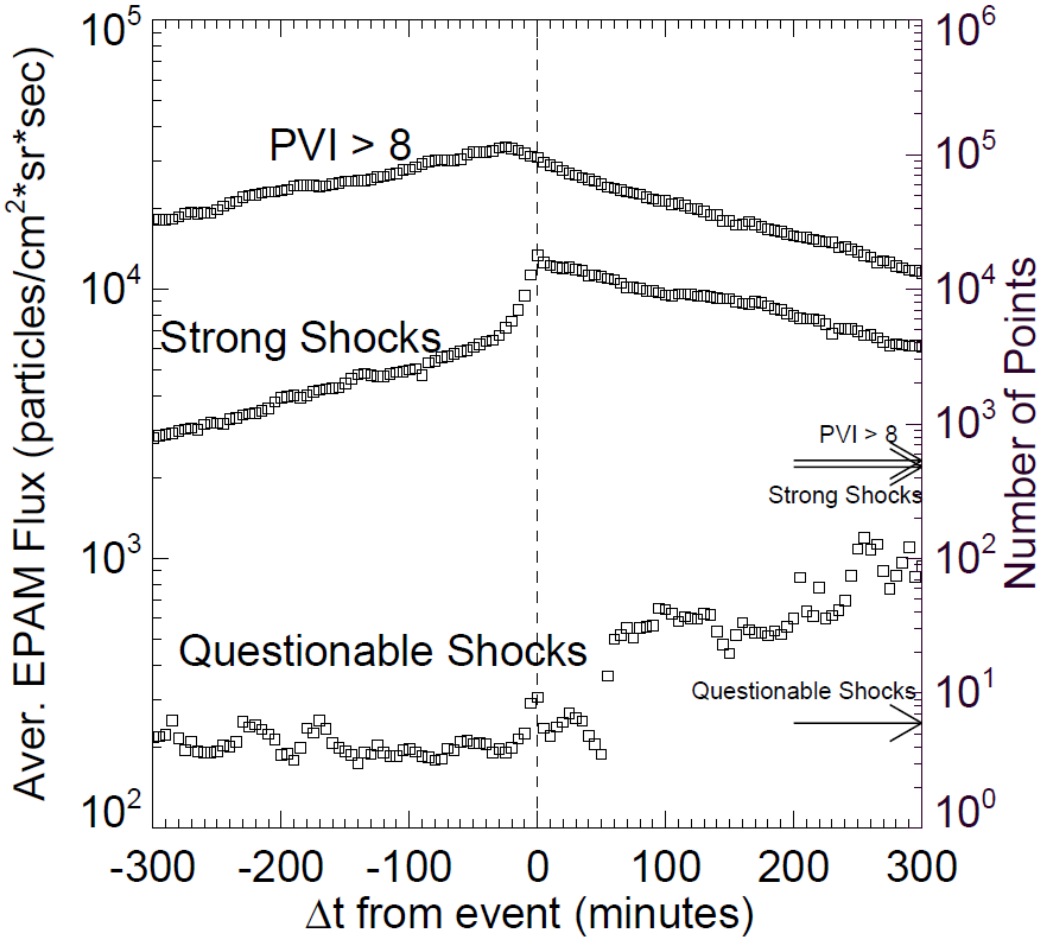

Tessein et al., ApJL, 2013

Complex Time-Intensity Profiles in Shock Acceleration

Matsumoto et al., Science, 2015

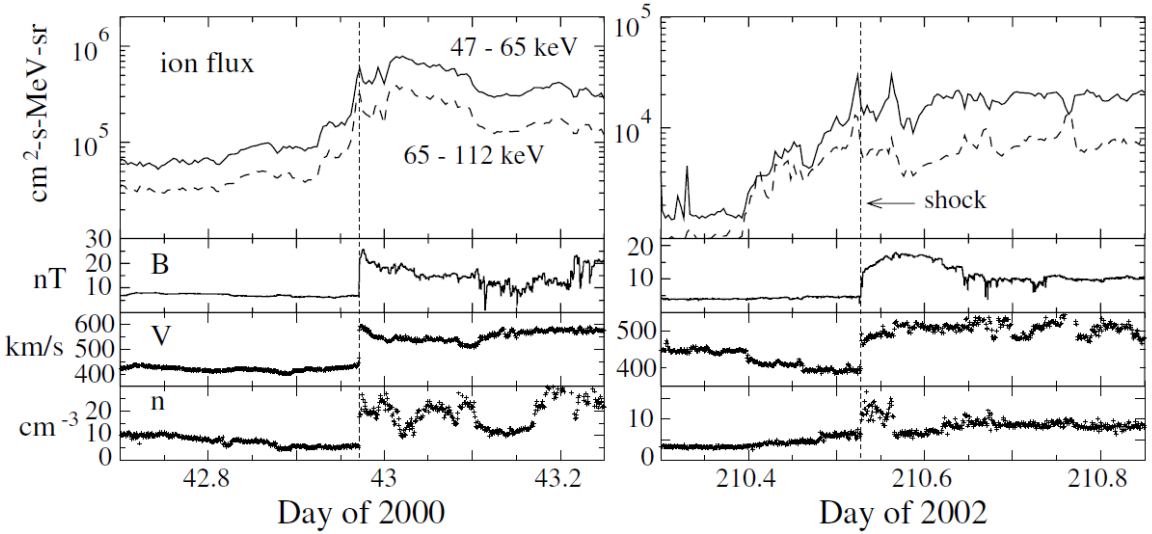

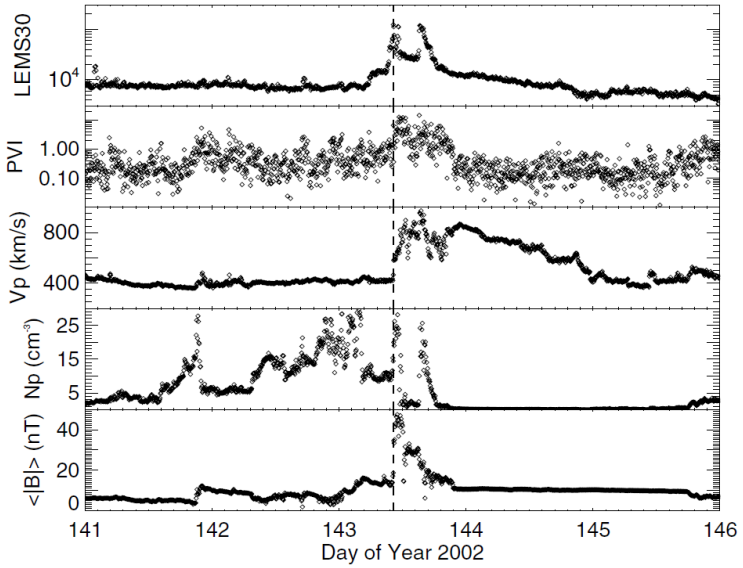

Above: Giacalone, ApJ, 2012

Left:Tessein et al. ApJL, 2013

Trapping in magnetic O-points

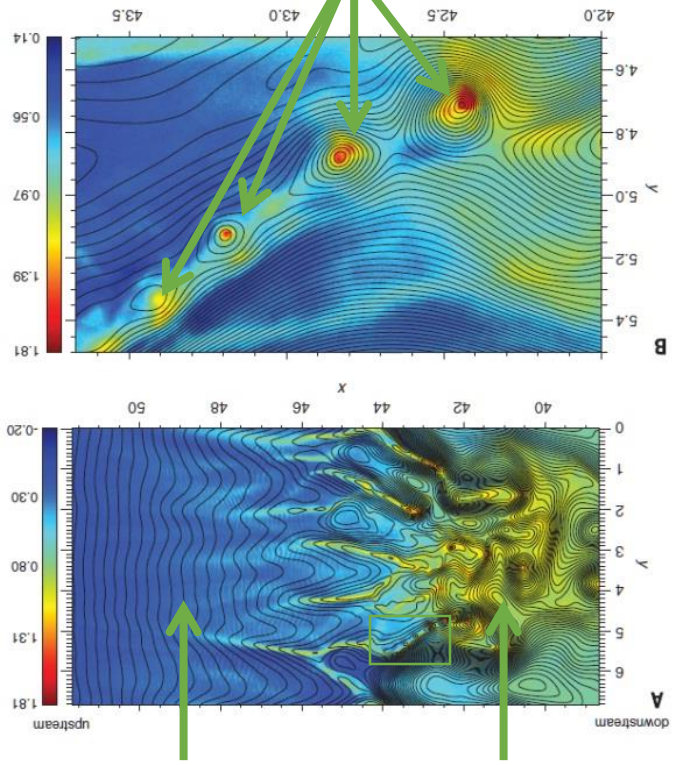

Unshocked region

Shocked region

Magnetic Reconnection

		Int. 1 (%)		Int. 2 (%)		Int. 3 (%)		Int. 4 (%)	
λ (%)	ζ	E_{RE}	E_{CS}	E_{RE}	E_{CS}	E_{RE}	E_{CS}	E_{RE}	E_{CS}
100	0	100	100	100	100	100	100	100	100
50	0.5	100	86.0	100	86.2	100	86.4	100	86.0
10	1.4	100	40.7	100	41.4	100	41.5	100	40.6
5	2.0	99.3	27.0	100	27.8	100	27.7	98.0	26.2
1	3.5	87.7	9.4	90.4	9.6	92.4	9.7	86.9	9.0
0.5	4.4	72.5	5.7	76.0	5.9	81.9	5.9	79.1	5.5
0.1	6.6	29.0	1.6	36.8	1.6	41.9	1.7	44.4	1.5
0.05	7.6	22.5	0.9	26.4	0.9	25.7	0.9	32.7	0.8
0.01	10.2	9.4	0.2	11.2	0.2	13.3	0.2	13.1	0.2
0.005	11.2	6.5	0.1	7.2	0.1	6.7	0.1	7.8	0.1
0.001	14.4	2.2	0.02	2.4	0.03	2.9	0.02	3.3	0.02
0.0005	15.8	1.4	0.007	0.8	0.01	1.9	0.01	2.0	0.01
0.0001	18.1	0.7	0.004	0.8	0.003	1.0	0.004	0.7	0.004

Osman et al., PRL 2014: 87%–92% of all reconnection exhausts and about 9% of all current sheets are concentrated within the highest 1% of PVI values

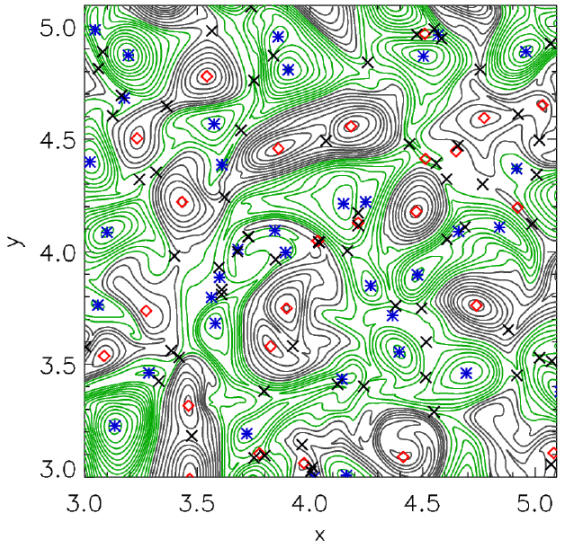

Servidio et al., JGR, 2011

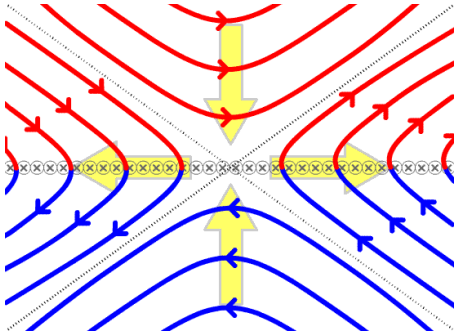

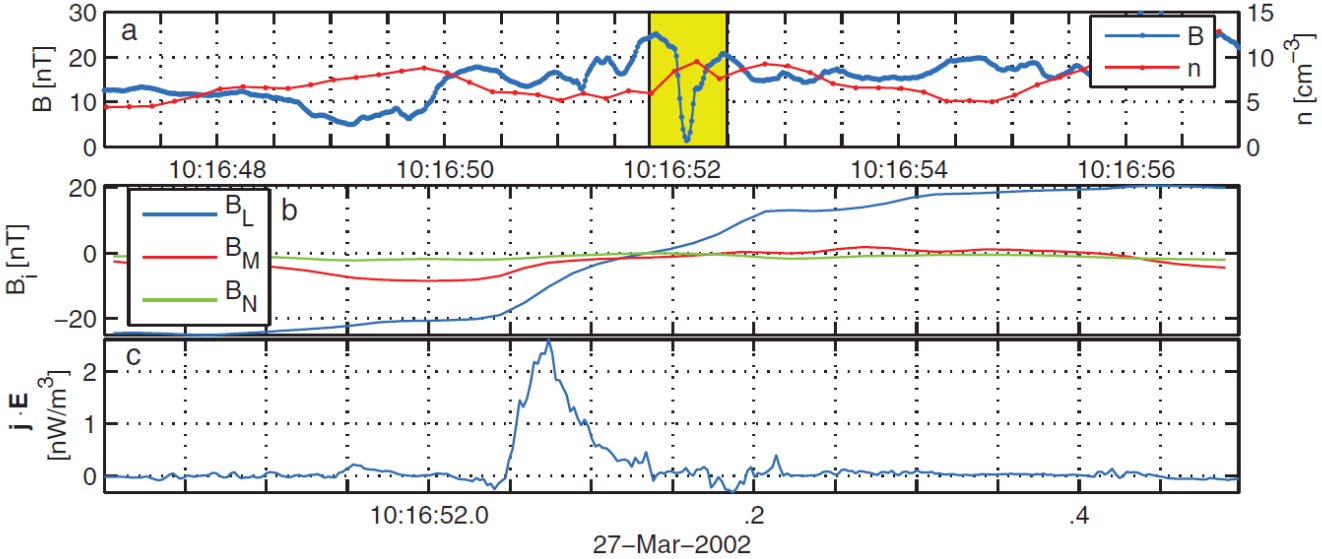

Sundkvist et al., PRL, 2007

Coherent Structures - Dissipation

- Most of the dissipation contained in a small percentage of the total volume (coherent structures)

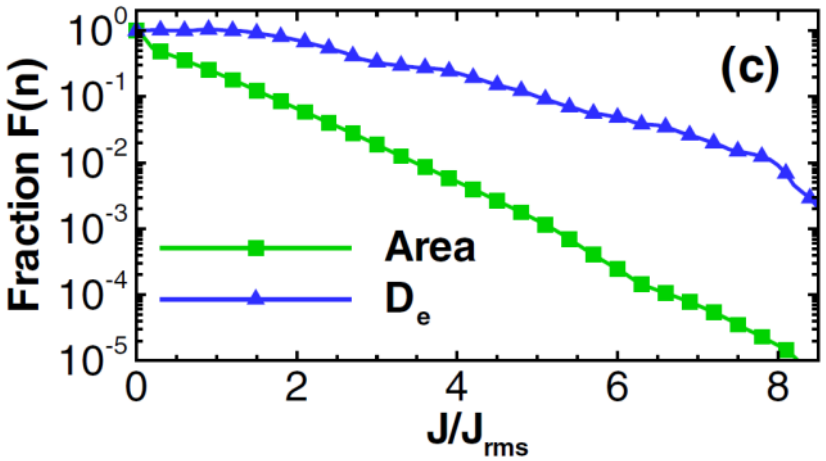

Wan et al., PRL 2012

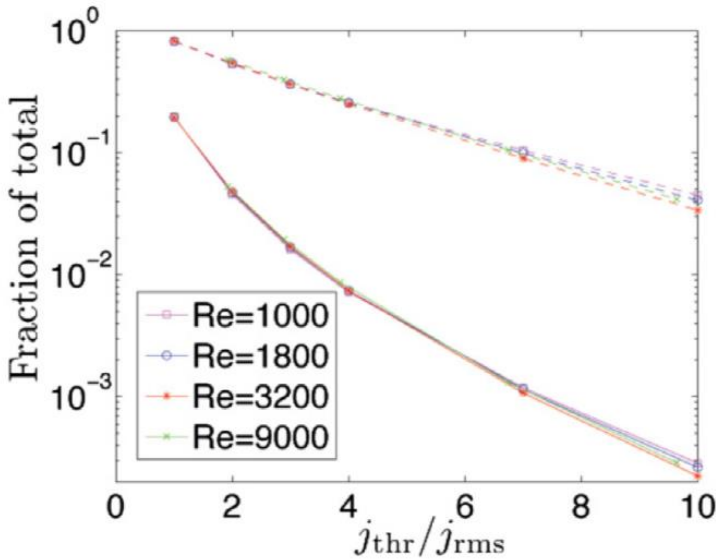

Zhdankin et al., ApJ, 2014

Coherent Structures - Instabilities

- Increased temperature and PVI associated with instability thresholds

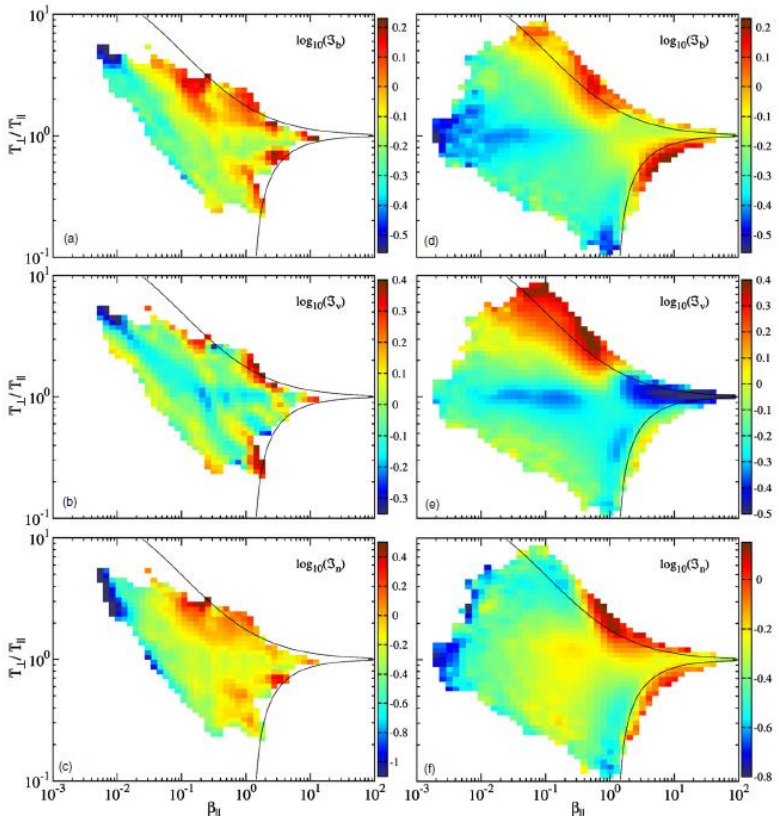

Servidio et al., ApJL, 2014

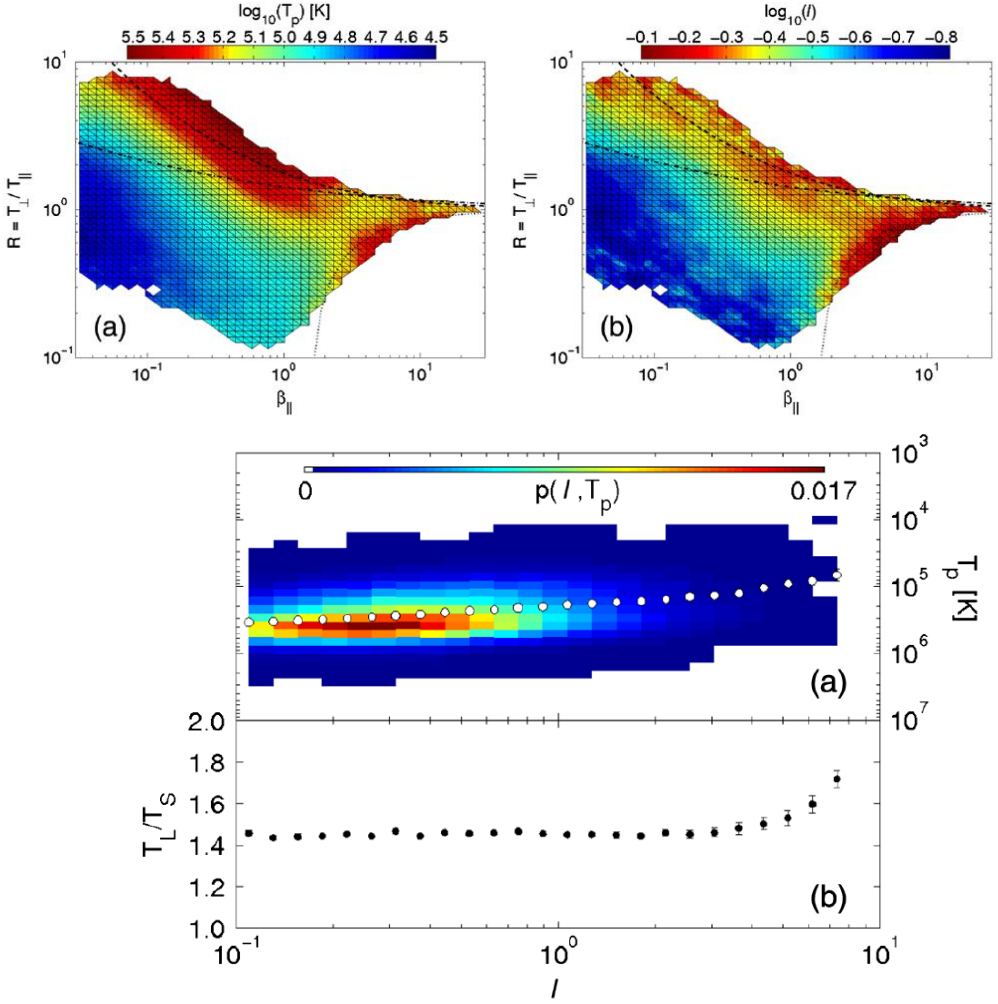

Osman et al., PRL, 2012

Prevalence of Coherent Structures in Shocked Regions

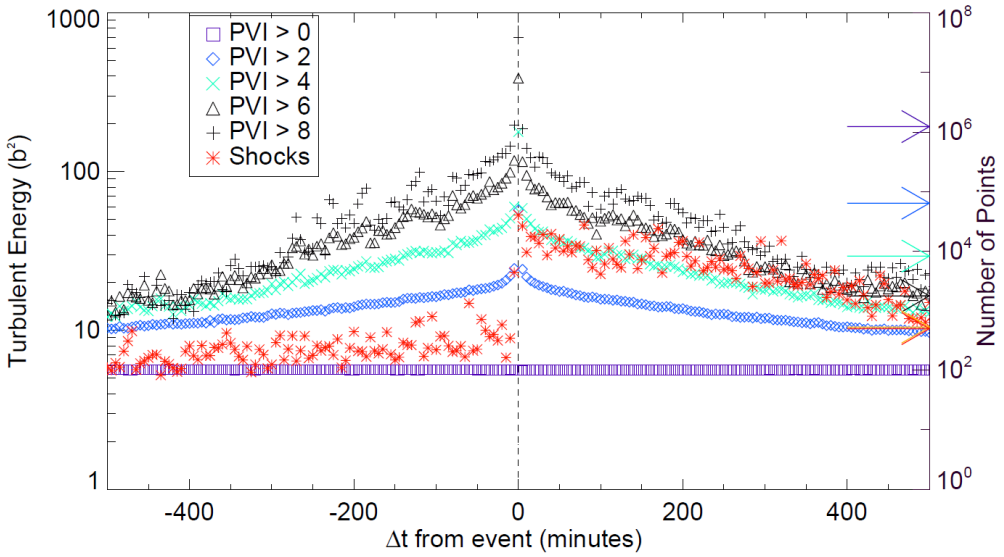

PVI can be thought of as a proxy for turbulence level

Caveat: Typically 1/5 of IP shocks are reverse shocks

Tessein et al., ApJ, 2015

Tangential Discontinuity (TD)

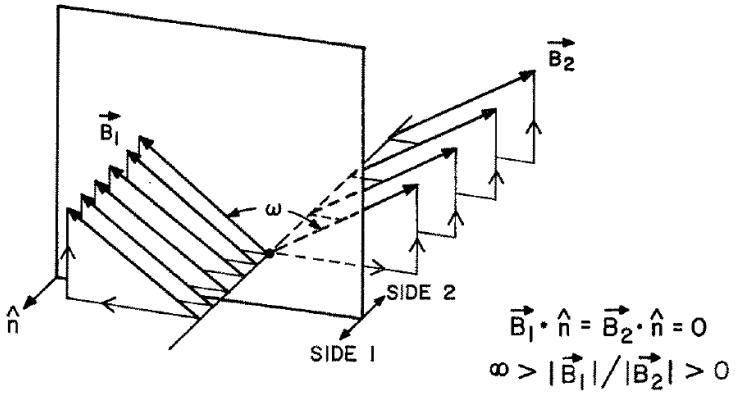

Burlaga & Ness 1969

Discontinuities

- A sudden change in the magnitude and/or direction of a field
- Various classifications, e.g. TD, RD
- Flux tube vs. in situ generation
- Coherent structures – Localized region of strong current (current sheet, magnetic discontinuity)

Borovsky, JGR, 2008

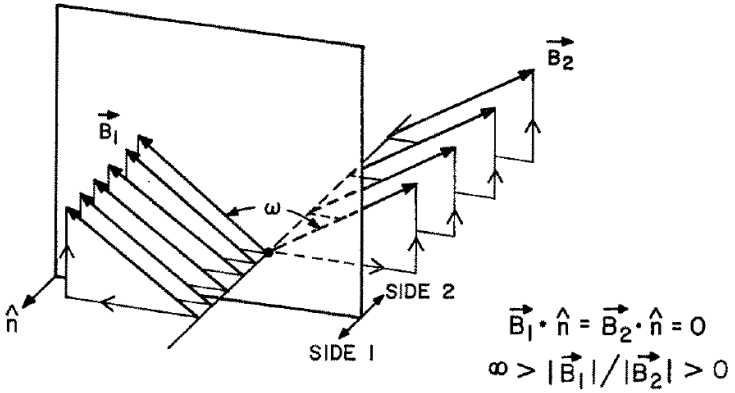

TD: Burlaga & Ness, SP, 1969

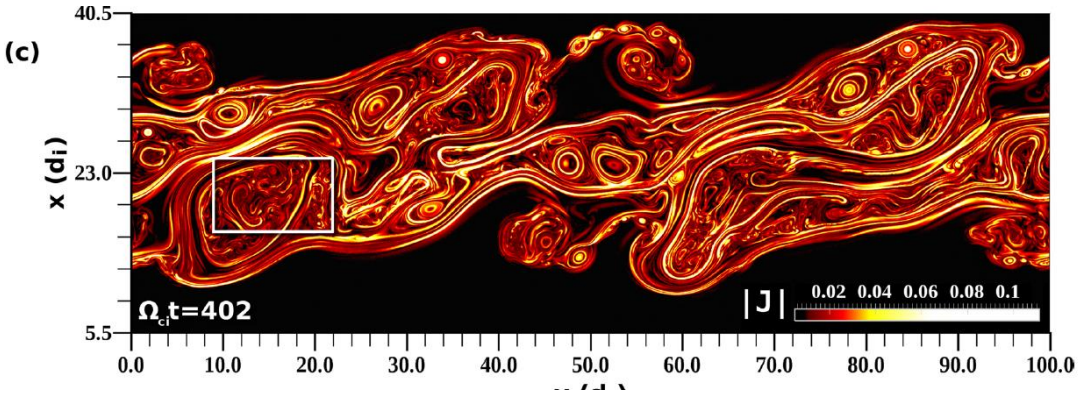

Kelvin-Helmholtz: Karimabadi et al., PoP, 2013

Shock PVI

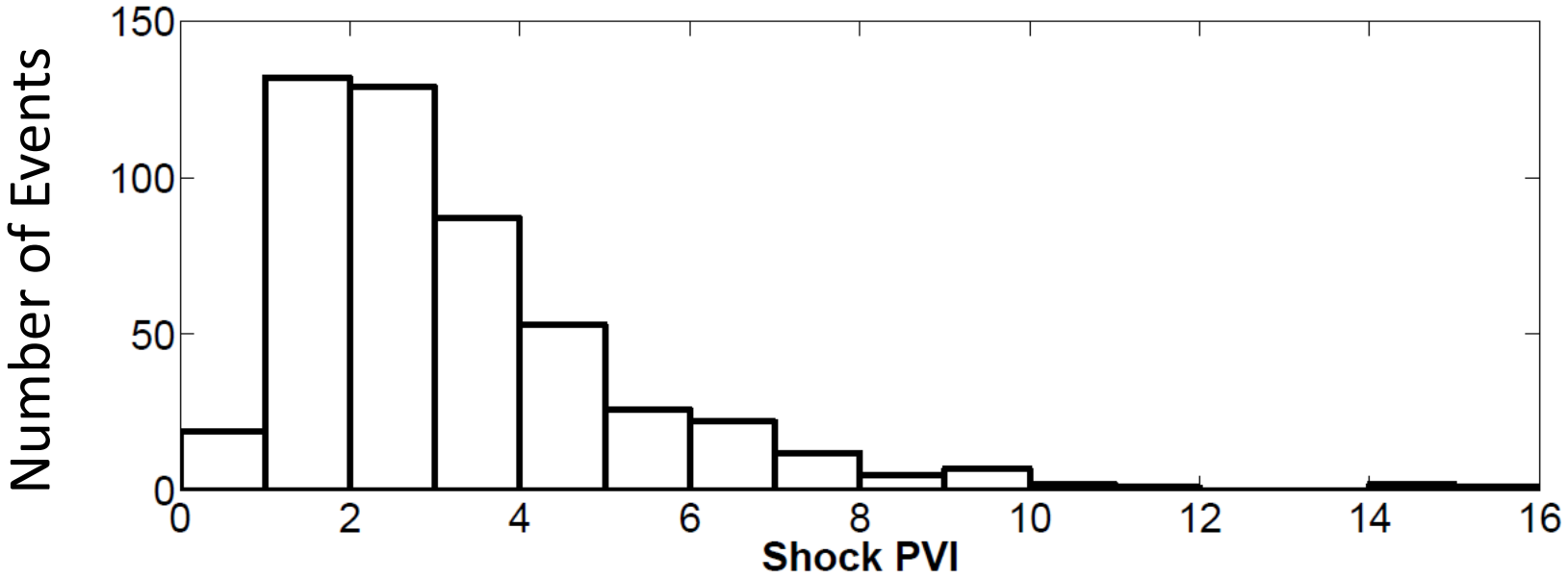

Histogram of the PVI value at 498 shocks. The shock-associated PVI value was obtained by taking the five nearest measurements to the shock (the nearest neighbor plus two on either side). Note that the distribution peaks for PVI < 2, which is a relatively low PVI value.

Complications of SEP Sources: Longitudinal spreading

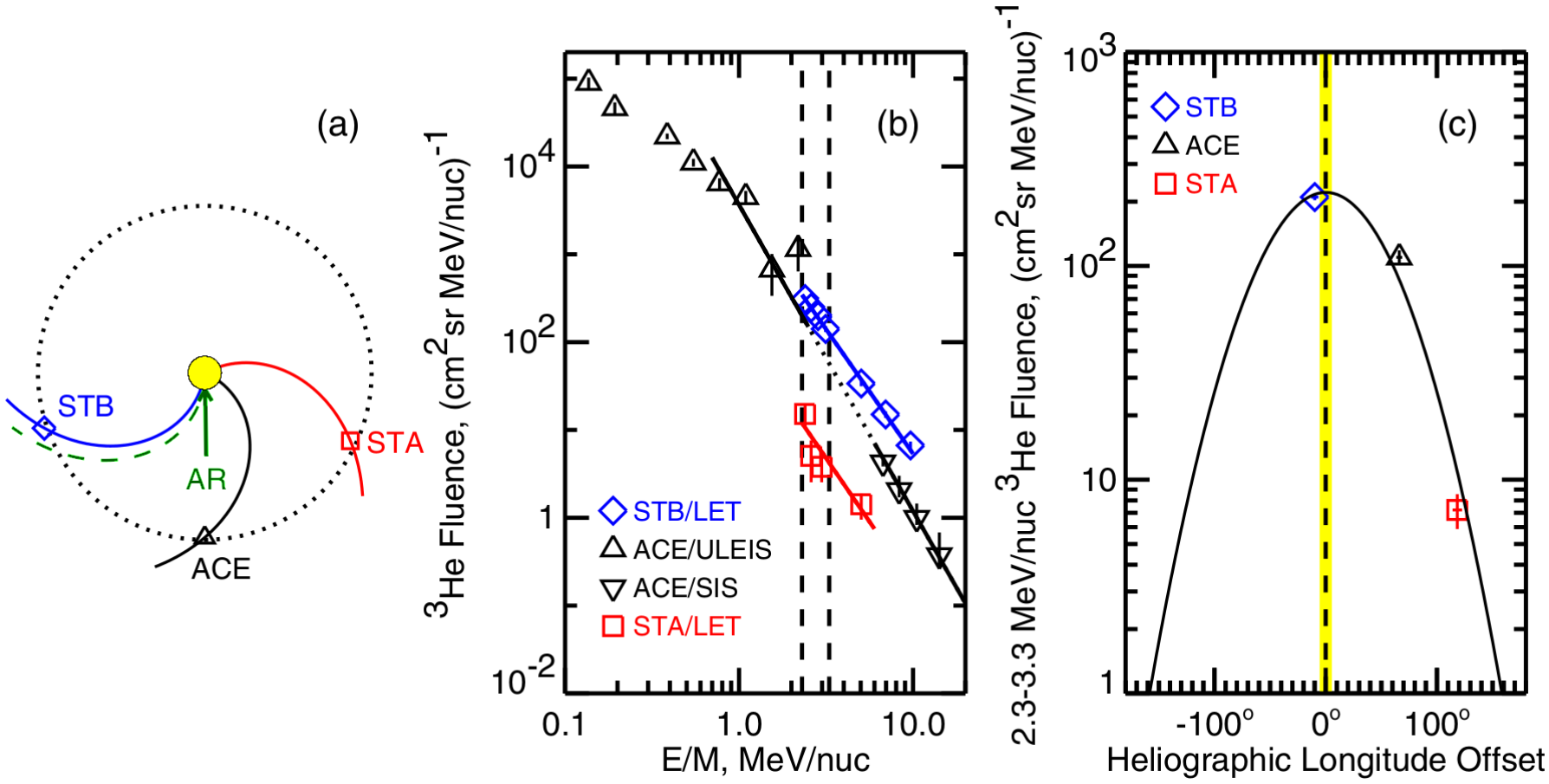

Wiedenbeck et al., ApJ, 2013

Complications of SEP Sources: Possible Resolution

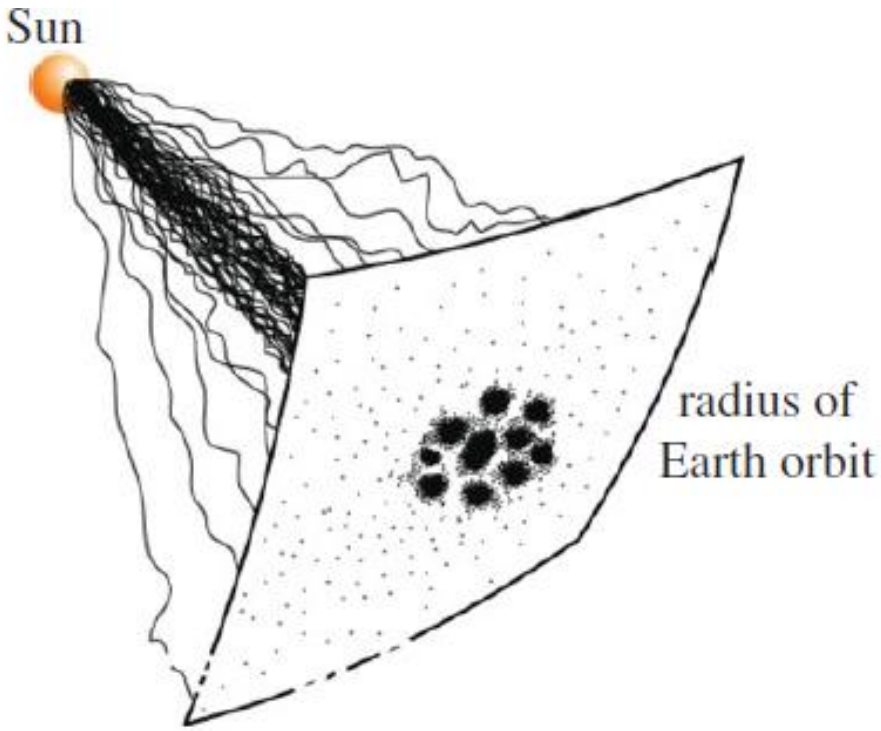

Ruffolo et al., ApJ, 2003

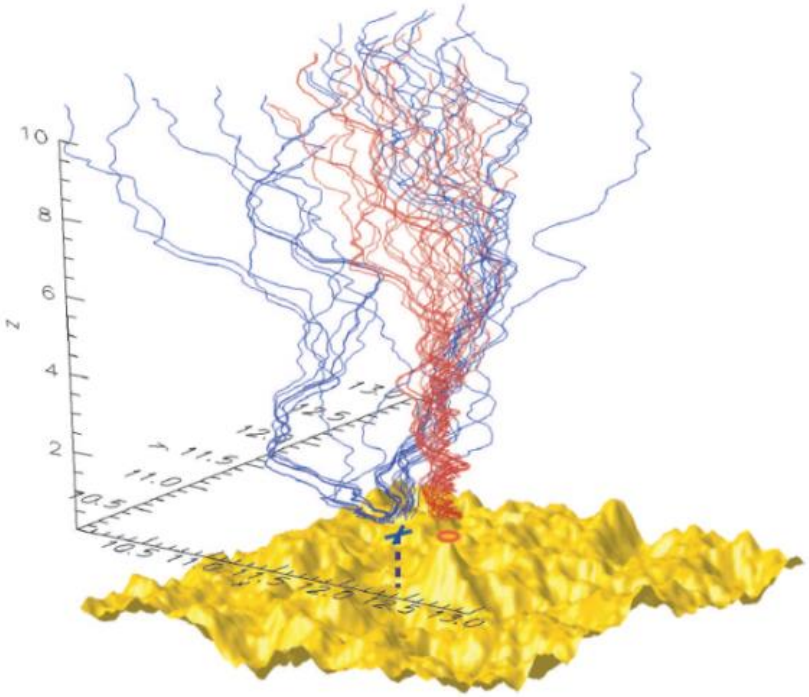

Chuychai et al., ApJ, 2007

Complications of SEP Sources: Dropouts

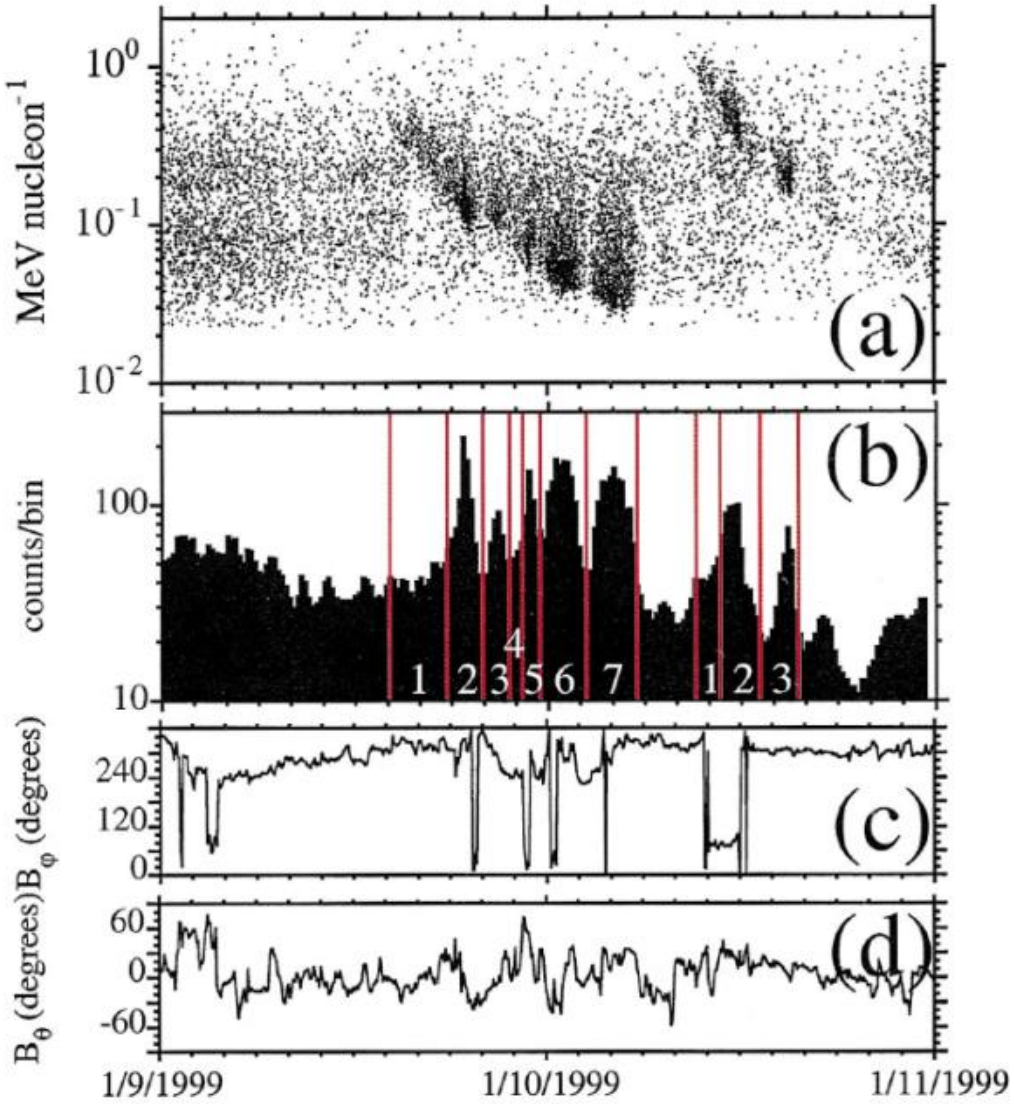

Mazur et al., ApJL, 2000

Coherent Structures and Energetic Particles

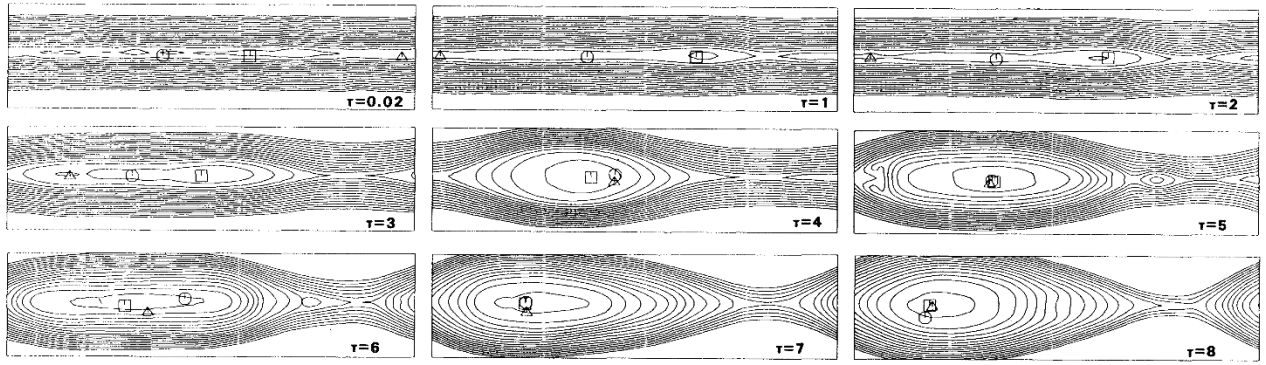

Matthaeus et al., PRL, 1984

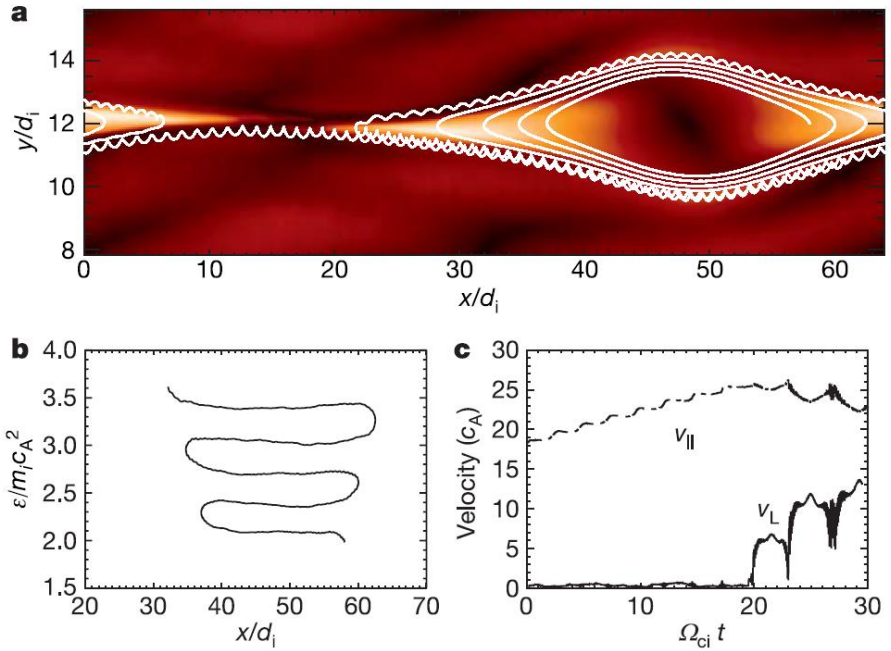

Drake et al., Nature, 2006

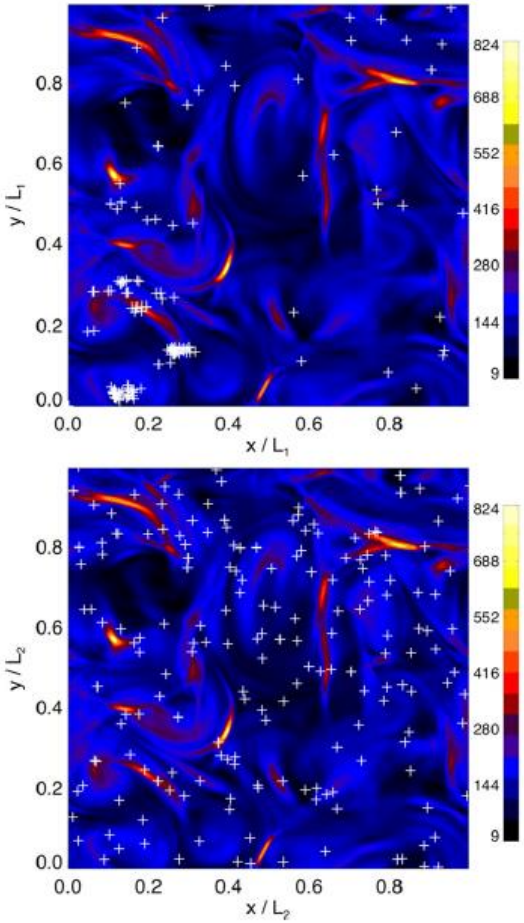

Dalena et al., ApJ, 2014

Acceleration Downstream of Shocks

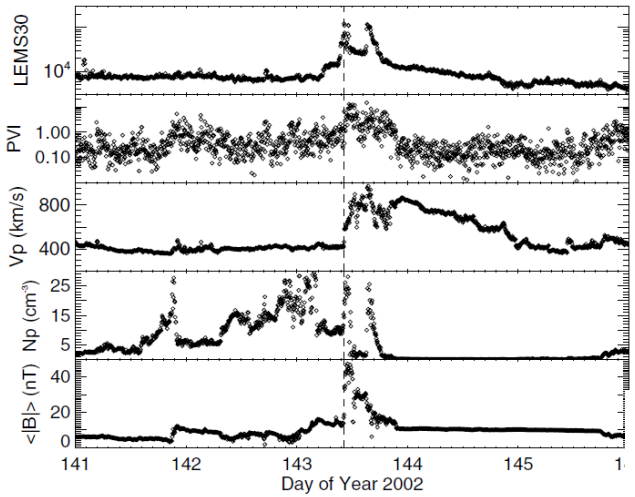

Tessein et al., ApJL, 2013

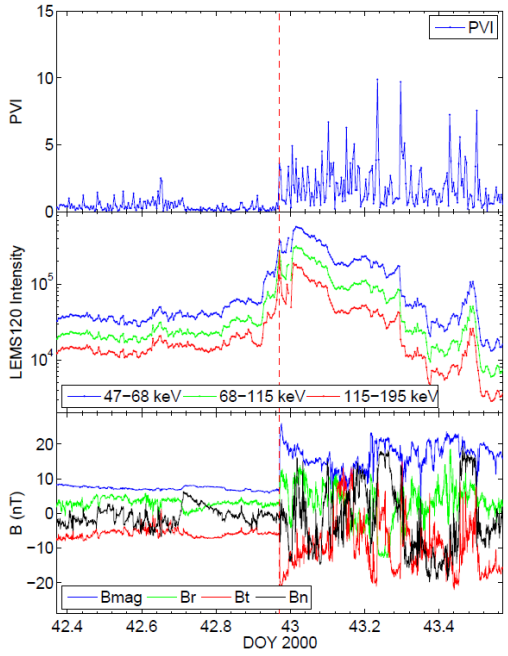

Location of PVI Events

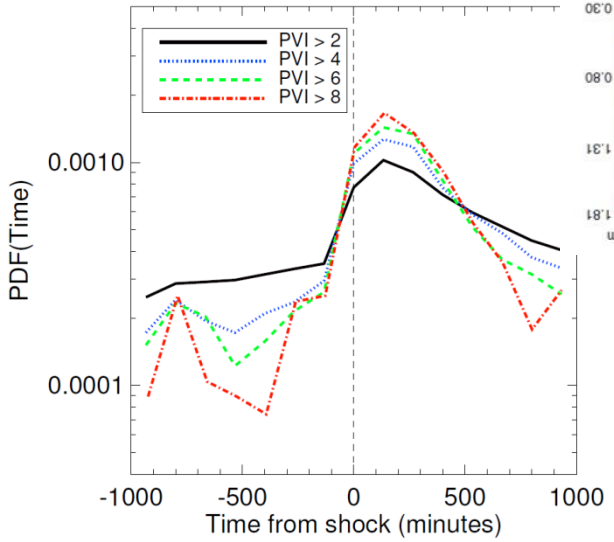

Trapping in magnetic O-points

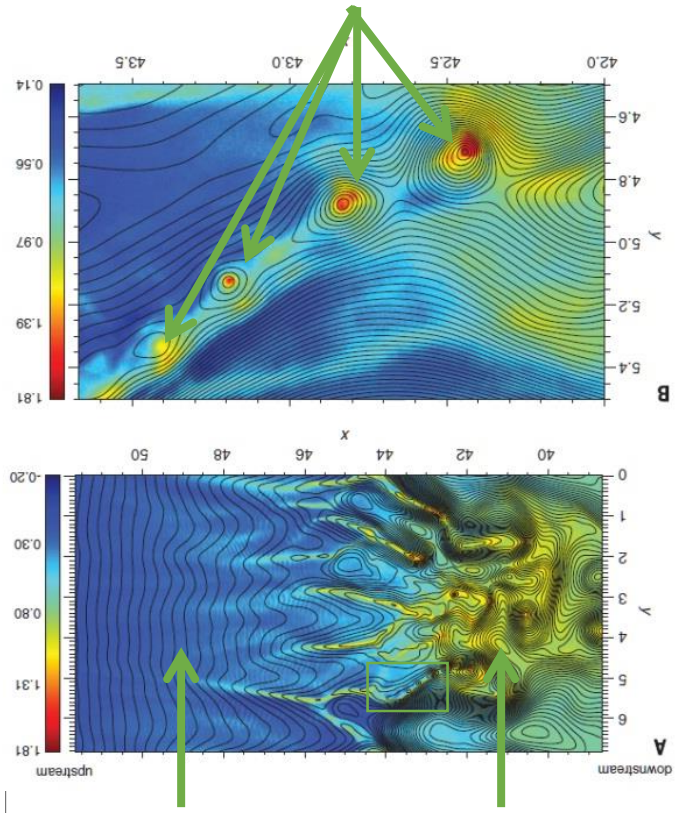

Matsumoto et al., Science, 2015

Lagged Cross Correlation

Correlation peaks at zero lag: Magnetic field and energetic particle intensity are often changing simultaneously – evidence in support of interpreting flux tubes as pipes

$$I'(t) = I(t) - \langle I \rangle$$
$$PVI'(t) = PVI(t) - \langle PVI \rangle,$$

$$C(I', PVI') = \frac{\langle I'(t) PVI'(t+\tau) \rangle}{\sqrt{\sigma_I \sigma_{PVI}}}$$

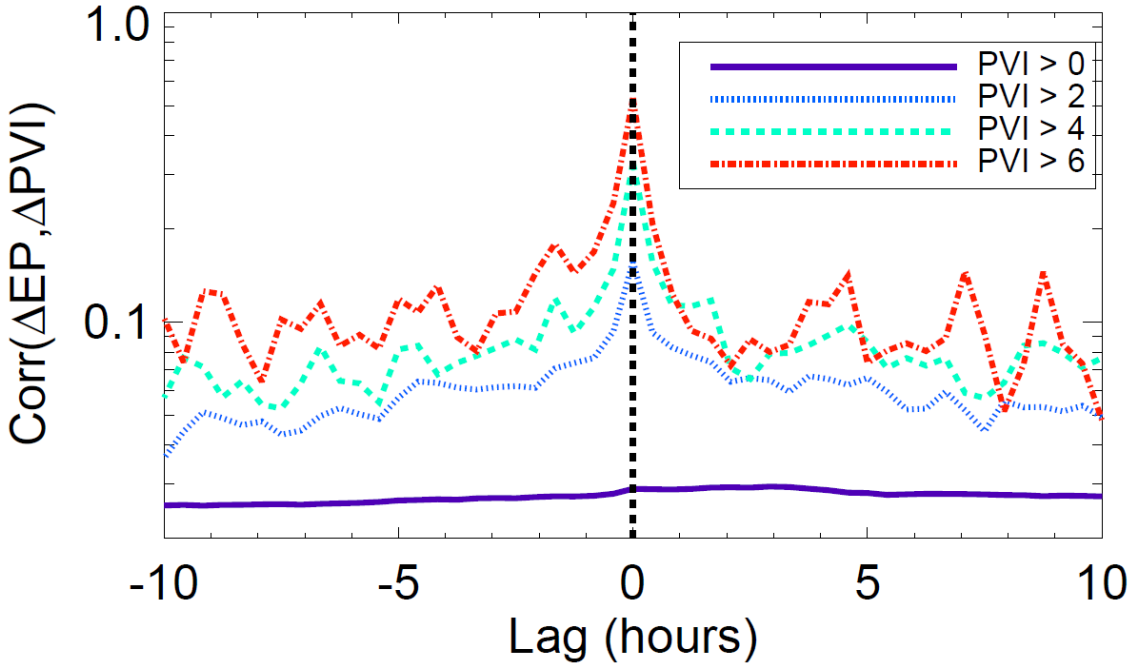

Tessein et al., ApJ, 2015

Diffusive Shock Acceleration

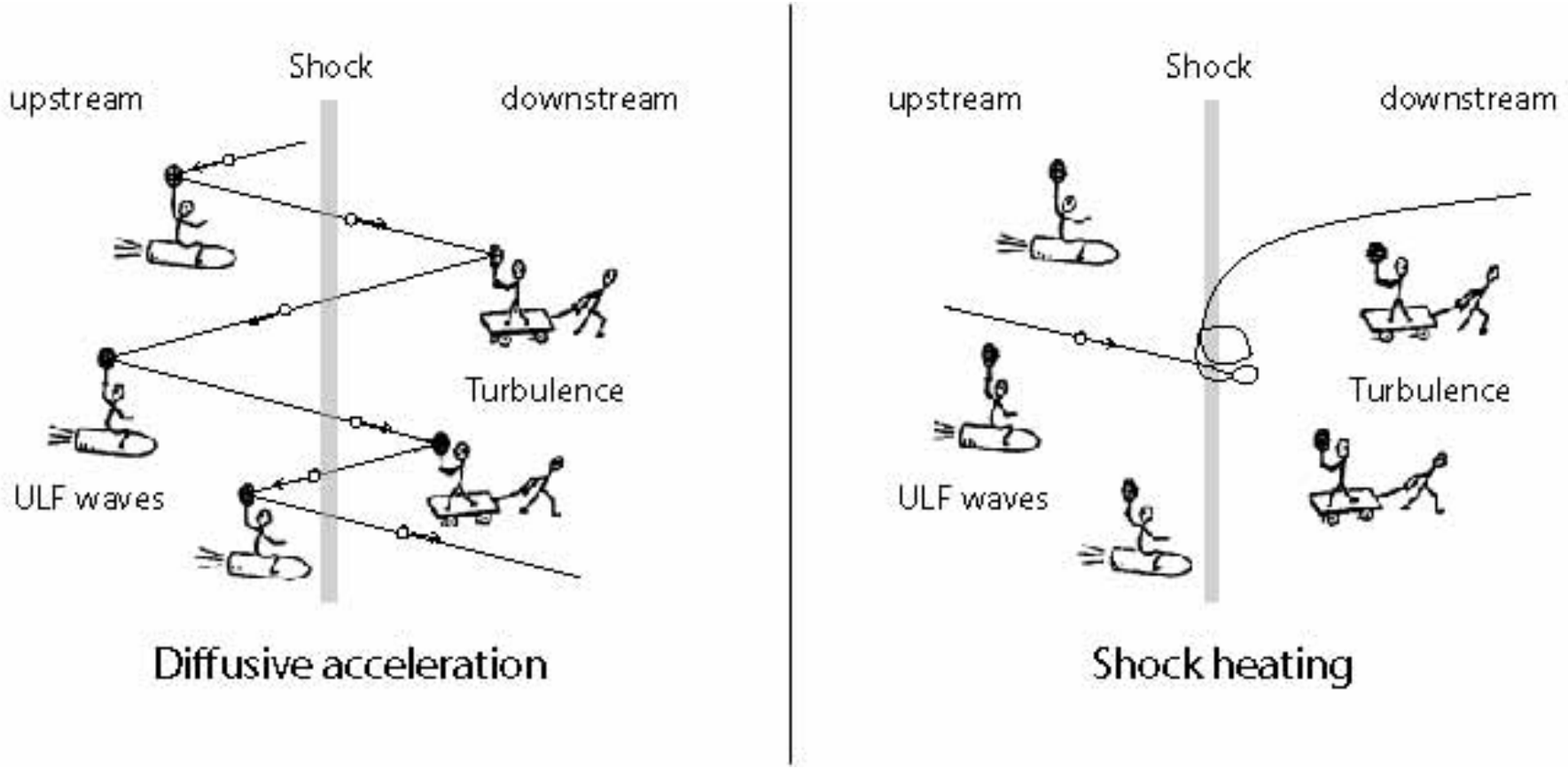

Treumann & Jaroschek, arXiv, 2008

Questions?